JPET Fast Forward. Published on August 21, 2024 as DOI: 10.1124/jpet.124.002184
This article has not been copyedited and formatted. The final version may differ from this version.

Recent Trends in the Pharmacology of Cardiovascular Diseases

Minireview

Drug-induced long QT syndrome: Concept and non-clinical models for predicting the onset of drug-induced torsade de pointes in patients in compliance with ICH E14/S7B guidance

Atsushi Sugiyama[1], Ai Goto[1], Hiroko Izumi-Nakaseko[1], Yoshinori Takei[1], Akira Takahara[2], Ryuichi Kambayashi[1]

[1]Department of Pharmacology, Faculty of Medicine, Toho University, 5-21-16 Omori-nishi, Ota-ku, Tokyo 143-8540, Japan

[2]Department of Pharmacology and Therapeutics, Faculty of Pharmaceutical Sciences, Toho University, 2-2-1 Miyama, Funabashi, Chiba 274-8510, Japan.

JPET Fast Forward. Published on August 21, 2024 as DOI: 10.1124/jpet.124.002184
This article has not been copyedited and formatted. The final version may differ from this version.

Running title:

Concept and models for drug-induced TdP

Corresponding author:

Atsushi Sugiyama, MD, PhD

Department of Pharmacology, Faculty of Medicine, Toho University

5-21-16 Omori-nishi, Ota-ku, Tokyo 143-8540, Japan

E-mail: atsushi.sugiyama@med.toho-u.ac.jp

The number of text pages: 34

The number of tables: 5

The number of figures: 5

The number of references: 159

The number of words in the abstract: 236

The number of words in the body of manuscript: 7,095

JPET Fast Forward. Published on August 21, 2024 as DOI: 10.1124/jpet.124.002184
This article has not been copyedited and formatted. The final version may differ from this version.

A list of nonstandard abbreviations:

AV: Atrioventricular

CSRC: Cardiac Safety Research Consortium

CiPA: Comprehensive In Vitro Proarrhythmia Assay

ECG: Electrocardiogram

FDA: Food and Drug Administration

HESI: The Health and Environmental Sciences Institute

iPS: Induced pluripotent stem

ICH: International Council for Harmonisation of Technical Requirements for Pharmaceuticals for Human Use

Q&As: Questions and answers

STV: Short-term variability

TQT: Thorough QT

TdP: Torsade de pointes

A recommended section assignment to guide the listing in the table of contents:

Cardiovascular

JPET Fast Forward. Published on August 21, 2024 as DOI: 10.1124/jpet.124.002184
This article has not been copyedited and formatted. The final version may differ from this version.

Abstract

ICH established S7B and E14 guidelines in 2005 to prevent drug-induced torsade de pointes (TdP), effectively preventing the development of high-risk drugs. However, those guidelines unfortunately hampered the development of some potentially valuable drug candidates despite not being proven to be proarrhythmic. In response, Comprehensive In Vitro Proarrhythmia Assay (CiPA) and Exposure-Response Modeling were proposed in 2013 to reinforce proarrhythmic risk assessment. In 2022, ICH released E14/S7B Q&As (Stage 1), emphasizing a "double negative" nonclinical scenario for low-risk compounds. For "non-double negative" compounds, new Q&As are expected to be enacted as Stage 2 shortly, in which more detailed recommendations for proarrhythmia models and proarrhythmic surrogate markers will be provided. This review details the onset mechanisms of drug-induced TdP, including I_{Kr} inhibition, pharmacokinetic factors, autonomic regulation and reduced repolarization reserve. It also explores the utility of proarrhythmic surrogate markers (J-T_{peak}, T_{peak}-T_{end} and terminal repolarization period) besides QT interval. Finally, it presents various in silico, in vitro, ex vivo and in vivo models for proarrhythmic risk prediction, such as CiPA in silico model, iPS cell-derived cardiomyocyte sheet, Langendorff perfused heart preparation, chronic atrioventricular block animals (dogs, monkeys, pigs and rabbits),

acute atrioventricular block rabbits, methoxamine-sensitized rabbits, and genetically engineered rabbits for specific long QT syndromes. Those models along with the surrogate markers can play important roles in quantifying TdP risk of new compounds, impacting late-phase clinical design and regulatory decision-making, and preventing adverse events on post-marketing clinical use.

Significance Statement

Since ICH S7B/E14 guidelines unfortunately hampered the development of some potentially valuable compounds with unproven proarrhythmic risk, Comprehensive In Vitro Proarrhythmia Assay and Exposure-Response Modeling were proposed in 2013 to reinforce proarrhythmic risk assessment of new compounds. In 2022, ICH released Q&As (Stage 1) emphasizing "double negative" nonclinical scenario for low-risk compounds, and new Q&As (Stage 2) for "non-double negative" compounds are expected. This review delves into proarrhythmic mechanisms with surrogate markers, and explores various models for proarrhythmic risk prediction.

Keywords

Comprehensive In Vitro Proarrhythmia Assay; ICH E14/S7B Q&As; Proarrhythmic surrogate marker; QT interval; Torsade de pointes

JPET Fast Forward. Published on August 21, 2024 as DOI: 10.1124/jpet.124.002184
This article has not been copyedited and formatted. The final version may differ from this version.

Introduction

The pathologic condition, in which some drugs prolong QT interval of electrocardiogram (ECG) and induce a lethal ventricular arrhythmia known as torsade de pointes (TdP), is called "drug-induced long QT syndrome"(Sugiyama, 2008; Kannankeril et al., 2010; Sager et al., 2014). To avoid such serious adverse events, International Council for Harmonisation of Technical Requirements for Pharmaceuticals for Human Use (ICH) signed the S7B and E14 guidelines as Step 4 in May 2005, clearly defining the content and role of non-clinical and clinical studies, respectively (Anonymous, 2005ab). After the S7B and E14 guidelines entered into force, the number of new drug candidates that would have the risk inducing TdP has decreased dramatically. On the other hand, it has also become clear that there were some potentially valuable drug candidates that tested positive for S7B or E14 and therefore discontinued from development, even though they are assumed to have no proarrhythmic effect (Sager et al., 2014). To address such issues, Cardiac Safety Research Consortium (CSRC) /The Health and Environmental Sciences Institute (HESI) /Food and Drug Administration (FDA)-led thinktank meeting was held in July 2013, in which a new paradigm for risk assessment of drug-induced arrhythmias was discussed, and Comprehensive In Vitro Proarrhythmia Assay (CiPA) and Exposure-Response

Modeling were proposed as a breakthrough (Darpo et al., 2014; Sager et al., 2014).

In February 2022, ICH released newly integrated guideline E14/S7B on clinical and nonclinical evaluation of QT/QTc interval prolongation and proarrhythmic potential - questions and answers - (ICH E14/S7B Q&As) (Anonymous, 2022), which consists of a revised Q&A for the E14 guideline and a new Q&A for the S7B guideline, bringing the cardiac safety evaluation of novel candidate compounds into a new phase. In these Q&As, guidelines for developing candidate compounds that show a low risk for arrhythmia have been compiled as Stage 1, in which the concept of a "double negative" nonclinical scenario consisting of the negative hERG assay and negative in vivo QTc study is introduced to demonstrate that a drug will not produce a clinically relevant QTc prolongation (Strauss et al., 2021; Rossman et al., 2023). Moreover, this nonclinical "double negative" data package along with negative phase I clinical QTc data; so-called "triple negative", is expected to be sufficient to substitute for a clinical Thorough QT (TQT) study in some specific cases (Strauss et al., 2021; Rossman et al., 2023). In contrast, new Q&As for "non-double negative" compounds are currently under discussion within the ICH E14/S7B working group, and are expected to be enacted as Stage 2 shortly, in which more detailed recommendations for the proarrhythmia models and proarrhythmic surrogate markers are provided.

In the original S7B 2.3.5 in 2005 (Anonymous, 2005a), as well as the new S7B Q&A 1.1 (Anonymous, 2022), proarrhythmia models/algorithms were described to be able to play a crucial role in the quantitative assessment of proarrhythmic risk of new drug candidates in a follow-up study, that will impact late-phase clinical design and regulatory decision-making (and labeling) on marketing application (Strauss et al., 2021; Rossman et al., 2023). However, information on the predictability, reproducibility and robustness of the in silico, in vitro and ex vivo proarrhythmia models (Hondeghem et al., 2001; Kannankeril et al., 2010; Ando et al., 2017; Li et al., 2019) as well as the in vivo models besides the proarrhythmic surrogate markers (Sugiyama 2008; Kannankeril et al., 2010; Johannesen et al., 2014ab; Loen et al., 2022) remains limited, since creating such information requires advanced clinical and experimental experiences as well as knowledge. Accordingly, there is a clear need to update those pieces of information to better understand and discuss the Q&As Stage 2. Over the past 30 years, we have been involved in the development of several in vitro and in vivo proarrhythmia models that can detect drug-induced repolarization delay and predict the onset of TdP arrhythmias in patients. The developed models have been used to quantify the magnitude of risk of various drugs/compounds for the onset of TdP and identify their safety margin (Sugiyama et al., 2002a, 2011; Sugiyama, 2008;

Nakamura et al., 2014; Izumi-Nakaseko et al., 2018; Goto et al., 2019b, 2020a, 2021, 2022). Therefore, we utilized this article to summarize recent insights into the onset mechanism of drug-induced long QT syndrome along with the integration of new findings on proarrhythmic surrogate markers as well as to consolidate the utility and limitations of currently available proarrhythmia models compliant with the ICH E14/S7B Q&As.

Onset mechanism of drug-induced TdP

Drug-induced inhibition of I_{Kr} in the heart is the primary cause of TdP arrhythmias. However, even when I_{Kr} is suppressed, QT-interval prolongation, as well as TdP, occurs in only a few patients (Fig. 1). In other words, the suppression of I_{Kr} is a necessary condition but is not sufficient for developing drug-induced TdP in most of the patients (Sugiyama, 2008). To overcome those challenges inherent in the in vitro I_{Kr} assay, animal models of TdP have been developed that possess a whole set of pathophysiology assumed to exist in the heart of patients developing drug-induced long QT syndrome. Indeed, some in vivo proarrhythmia models have been used in safety pharmacology studies of new drug candidates. Each step of mechanisms toward the onset of TdP as indicated in Fig. 2 needs to be understood to properly select and use

JPET Fast Forward. Published on August 21, 2024 as DOI: 10.1124/jpet.124.002184
This article has not been copyedited and formatted. The final version may differ from this version.

each proarrhythmia model.

Distribution of drugs to the heart: The degree of drug-induced QT-interval prolongation is reflected more accurately in the following order: the number of ventricular K^+ channels blocked >drug concentration in the myocardial cells >plasma drug concentration. Thus, even if a drug potently inhibits I_{Kr} in the in vitro assay, its risk for inducing QT-interval prolongation and TdP may become very small when the drug is not sufficiently distributed to the heart due to rapid drug metabolism/excretion and/or very low lipophilicity (Goto et al., 2020a) (Fig. 2). Accordingly, a compound with such pharmacokinetic and/or physicochemical characteristics as described above may become a therapeutic agent with minimal adverse effects on the heart if it is a non-cardiovascular agent. In contrast, its usefulness will be limited if it is an antiarrhythmic agent used to treat ventricular arrhythmias.

Autonomic regulation of the heart: The autonomic nervous system distributed in the heart is involved in the development of drug-induced TdP. When an I_{Kr} blocker possesses additional vasodilator action, it decreases the blood pressure in vivo, inducing a reflex-mediated increase of sympathetic tone, which increases the heart rate along with physiological I_{Ks} current enhancement. In addition, I_{Ks} is activated by an increase of cyclic AMP resulting from the increased sympathetic tone even when the

heart rate is not changed (Marx et al., 2002). If the administered I_{Kr} blocker also inhibits the inward currents like I_{CaL} and I_{NaL}, these latter inhibitory actions along with the sympathetic tone-dependent enhancement of I_{Ks} may counterbalance the effect of I_{Kr} inhibition on the ventricular repolarization period, resulting in a small change in QT interval in the in vivo heart (Fig. 3). Thus, when evaluating the proarrhythmic effects of drugs/compounds in vivo, the modulation of the autonomic nervous system should always be considered along with their modulatory effects on each ionic current.

Reduced ventricular repolarization reserve: I_{Kr} inhibitors-induced excessive QT-interval prolongation tends to occur in pathological hearts, whereas intact monkeys and dogs are known to be 2- to 3-fold less sensitive than healthy humans (Sugiyama, 2008; Watson et al., 2011; Gotta et al., 2015; Komatsu et al., 2019; Chui et al., 2021; Vargas et al., 2023), which has been explained by the concept of "reduced repolarization reserve" (Sugiyama, 2008; Kannankeril et al., 2010; Varró and Baczkó, 2011) (Fig. 4). A reduction in the density of ventricular K^+ channels is the most representative example to constitute the body of the pathology. Since in the normal canine and monkey heart, K^+ channels are assumed to exist at more than twice the density required to maintain physiological repolarization (Sugiyama, 2008), the QT-interval prolongation is unlikely to occur even if K^+ channels are somewhat suppressed by drugs or hypokalemia. In

JPET Fast Forward. Published on August 21, 2024 as DOI: 10.1124/jpet.124.002184
This article has not been copyedited and formatted. The final version may differ from this version.

other words, the greater the density of K^+ channels, the greater their ability to maintain QT interval within the normal range; meaning the presence of a large repolarization reserve. This is the key role of the repolarization reserve in maintaining the homeostasis of the repolarization process. Meanwhile, in pathological conditions including chronic heart failure and genetic variation in certain cardiac K^+ channels (i.e. high-risk patients), net K^+ channel density is reduced, and QT interval is easily prolonged by I_{Kr} inhibitors and/or hypokalemia.

Further molecular mechanisms in repolarization reserve are presented here. Ventricular repolarization is orchestrated by the balanced activity of several inward and outward currents, which flow through different ionic channels, and electrogenic ionic exchangers and pumps. These include I_{NaL}, I_{CaL}, I_{to}, I_{Kr}, I_{Ks}, I_{K1}, I_{NCX} and $I_{Na/K}$. When the inward currents I_{NaL} and I_{CaL} increase within the physiological range, the plateau voltage will be shifted toward a more positive direction. This shift enhances outward K^+ currents, acting as a negative feedback mechanism. For another example, if repolarization is lengthened due to drug-induced I_{Kr} block, hypokalemia, genetic abnormality or bradycardia, the subsequent increase in the action potential duration would favor I_{Ks} activation, which provides a negative feedback mechanism. However, repolarization process becomes vulnerable to the QT-interval prolongation when there is

JPET Fast Forward. Published on August 21, 2024 as DOI: 10.1124/jpet.124.002184
This article has not been copyedited and formatted. The final version may differ from this version.

a significant augmentation of depolarizing factors (I_{NaL}, I_{CaL}, I_{NCX}) or a marked reduction in repolarizing factors (I_{Ks}, I_{K1}, $I_{Na/K}$). Under such conditions, even a slight decrease in I_{Kr} may lead to a significant prolongation of QT interval (Varró and Baczkó, 2011).

With the progress in understanding the concept of repolarization reserve, pharmacological recovery of repolarization reserve can become a possible therapeutic option to reduce the risk of TdP. For instance, long-term blockade of L/N-type Ca^{2+} channels by cilnidipine was reported to be able to ameliorate the ventricular electrical remodeling that occurred in the chronic atrioventricular (AV) block canine hearts via the recovery of repolarization reserve, of which underlying mechanism is assumed to be the suppression of the renin-angiotensin-aldosterone system (Takahara et al., 2009). A similar pharmacological efficacy of cilnidipine has been reported in chronic dialysis patients (Cao et al., 2017; Iida et al., 2017). Cilnidipine treatment for ≥4 weeks inhibited the QT-interval prolongation induced by dialysis; moreover, it shortened the basal QT interval before the hemodialysis.

Temporal dispersion of ventricular repolarization process: The occurrence of ventricular premature beats can be predicted by using an early repolarization period (Johannesen et al., 2014ab; Hagiwara-Nagasawa et al., 2021a). This early

repolarization period can be estimated by J-T_{peak} interval of ECG, which corresponds to phase 2 of action potential (Fig. 3). Net effect of the drug on inward (I_{NaL}, I_{CaL}) and outward (I_{Ks}, I_{Kr}) currents is mainly reflected in J-T_{peak} interval. Prolongation of J-T_{peak} interval eventually causes myocardial Ca^{2+} overload, which increases the temporal heterogeneity of repolarization, inducing early afterdepolarization and ventricular premature beats, a trigger for TdP (Fig. 2).

Involvement of I_{NCX} and I_{K1} in the temporal dispersion of repolarization process also deserves comment. Na^+/Ca^{2+} exchanger transports 3 Na^+ in exchange for 1 Ca^{2+} per cycle, producing a current (I_{NCX}). I_{NCX} is outward at the beginning of action potential when $[Ca^{2+}]_i$ is low and membrane potential is positive, whereas it becomes inward during the latter plateau phase, in early and late repolarization, and also during diastole. Under the condition of Ca^{2+} overload, the Na^+/Ca^{2+} exchanger drives a more depolarizing current that may provoke early/delayed afterdepolarization leading to the onset of premature ventricular contraction (Varró and Baczkó, 2011). Meanwhile, I_{K1} contributes to the repolarization process during phases 3 and 4 of the action potential, offsetting the depolarization induced by Ca^{2+} overload-induced early afterdepolarization (Varró and Baczkó, 2011).

The temporal heterogeneity can be quantified by using the beat-to-beat,

short-term variability (STV) of ventricular repolarization, reflecting alterations of intracellular Ca^{2+} cycling (Thomsen et al., 2004; Takahara et al., 2006; Varró and Baczkó, 2011). Poincaré plot is created by plotting the QT_n and QT_{n+1} values measured from the ECG waveforms of N+1 of consecutive ventricular beats on the horizontal and vertical axes, respectively. The STV obtained by the following equation is used as an index of temporal heterogeneity.

$$STV = \sum_{i=1}^{N} \left(|QT_{i+1} - QT_i| / [\mathrm{N} \times \sqrt{2}] \right)$$

STV has been used to differentiate the dangerous QT-interval prolongation from the relatively safe QT-interval prolongation (Takahara et al., 2008).

Spatial dispersion of ventricular repolarization process: Spatial electrical instability of the ventricle can be estimated by using the late repolarization period. This late repolarization period corresponds to T_{peak}-T_{end} interval of ECG (Fig. 3) (Johannesen et al., 2014ab; Hagiwara-Nagasawa et al., 2021a). Since I_{Kr} is the most important current responsible for phase 3 repolarization, its inhibition prolongs T_{peak}-T_{end} interval (Fig. 3 middle top). Prolongation of T_{peak}-T_{end} interval also indicates increased transmural dispersion of ventricular repolarization, which means that the coexistence time of ventricular cells, that have completed repolarization and those that have not, is prolonged, globally increasing ventricular electrical vulnerability (Shimizu

and Antzelevitch, 1997) (Fig. 3, middle bottom). Thus, measurement of T_{peak}-T_{end} interval allows quantification of spatial heterogeneity of the repolarization process of the ventricular wall. Since the onset time point of R on T-type ventricular premature beats induced by the drug-induced QT-interval prolongation usually coincides with phase 3 of the action potential (also corresponding to T_{peak}-T_{end} interval), the increase of spatial heterogeneity of the ventricle will facilitate the initiation of spiral re-entry, leading to the onset of TdP (Fig. 2).

Local electrical vulnerability for perpetuating spiral re-entry: The terminal repolarization period (TRP) of the ventricle is difference between the duration of monophasic action potential and the ventricular effective refractory period, which are usually assessed at the same site with a basic ventricular pacing cycle length of 400 ms (Sugiyama, 2008). Prolongation of TRP by I_{Kr} inhibitors facilitates the entrance of excitation originating from premature contraction or re-entry circuit at a less complete repolarization level, which could reflect the magnitude of local electrical vulnerability during ventricular tachycardia, providing a "substrate" for the perpetuation of spiral re-entry (Sugiyama and Hashimoto, 2002).

Validation of the J-T_{peak}, T_{peak}-T_{end} and TRP as proarrhythmic surrogate markers

JPET Fast Forward. Published on August 21, 2024 as DOI: 10.1124/jpet.124.002184
This article has not been copyedited and formatted. The final version may differ from this version.

Since the QT-interval prolongation by itself may not necessarily predict the onset of TdP (Sugiyama, 2008; Johannesen et al., 2014ab; Strauss et al., 2021), we have proposed to utilize the J-T_{peak}, T_{peak}-T_{end} and TRP in combination besides QT interval for non-clinical in vivo cardiac safety evaluation of drugs/compounds. Effects of antiarrhythmic agents (8 compounds), tyrosine kinase inhibitors (4 compounds), antiviral drugs (5 compounds) and psychotropic drugs (6 compounds) on the QTcV (QT interval corrected with Van de Water's formula) (Van de Water et al., 1989), J-T_{peak}c (J-T_{peak} corrected with Johannesen's formula) (Johannesen et al., 2014b), T_{peak}-T_{end} and TRP assessed in the halothane- or isoflurane-anesthetized dogs (in vivo QTc model) are summarized in Table 1 along with TdP risk categories obtained from the chronic AV block dogs (Table 2) and monkeys (Table 3) as well as CredibleMeds® which is an online database of drugs and drug-drug interactions that cause the QT-interval prolongation and TdP (Woosley et al., accessed 2024).

Antiarrhythmic agents: Based on the TdP risk categories from the chronic AV block dogs and/or CredibleMeds, all antiarrhythmic agents except for vanoxerine were described to induce the QT-interval prolongation and/or TdP to varying degrees (Table 1). Meanwhile, until recently vanoxerine was believed to become an efficacious and safe anti-atrial fibrillatory drug (Obejero-Paz et al., 2015). However, in a phase III

JPET Fast Forward. Published on August 21, 2024 as DOI: 10.1124/jpet.124.002184
This article has not been copyedited and formatted. The final version may differ from this version.

trial for patients with atrial fibrillation, 3 of the first 26 patients developed TdP (Piccini et al., 2016). Here, we discuss the proarrhythmic risk of vanoxerine along with the other 7 antiarrhythmic agents. Each agent prolonged QTcV to varying degree. The magnitude of change in J-T_{peak}c was comparable among vanoxerine, *dl*-sotalol, bepridil and vernakalant, which was greater than those by ranolazine, dronedarone and amiodarone, but smaller than that by E-4031. These findings suggest that vanoxerine, as well as *dl*-sotalol, bepridil and vernakalant, would have a larger risk to induce intracellular Ca^{2+} overload than ranolazine, dronedarone and amiodarone, but possess smaller risk compared with E-4031. The magnitude of change in T_{peak}-T_{end} was comparable among vanoxerine, *dl*-sotalol, amiodarone and bepridil, which was greater than that by ranolazine, but smaller than those by E-4031, vernakalant and dronedarone. These findings suggest that vanoxerine, as well as *dl*-sotalol, amiodarone and bepridil, would have a smaller risk to produce the substrate for initiation of spiral re-entry than E-4031, vernakalant and dronedarone, but possess a larger risk compared with ranolazine.

It is noteworthy that vanoxerine, *dl*-sotalol, bepridil and E-4031 prolonged J-T_{peak}c approximately 2 times greater than T_{peak}-T_{end} (J-T_{peak}c >T_{peak}-T_{end} pattern). In the risk classification with chronic AV block dogs, E-4031 and *dl*-sotalol are classified

JPET Fast Forward. Published on August 21, 2024 as DOI: 10.1124/jpet.124.002184
This article has not been copyedited and formatted. The final version may differ from this version.

into “high risk”, and bepridil is done into “intermediate risk”, whereas no information is available for vanoxerine. In the information of CredibleMeds, *dl*-sotalol and bepridil are classified into “known risk of TdP”, whereas no information is available for vanoxerine or E-4031. Vernakalant and ranolazine prolonged J-T_{peak}c and T_{peak}-T_{end} to a similar extent (J-T_{peak}c =T_{peak}-T_{end} pattern), whereas amiodarone and dronedarone prolonged J-T_{peak}c less potently than T_{peak}-T_{end} (J-T_{peak}c <T_{peak}-T_{end} pattern). In the risk classification with chronic AV block dogs, amiodarone and dronedarone are classified into “low/no risk” and “low/no risk (tentative)”, respectively, whereas no information is available for vernakalant or ranolazine. In the information of CredibleMeds, vernakalant is classified into “possible risk of TdP”, and ranolazine is done into “conditional risk of TdP”, although amiodarone and dronedarone are done into “known risk of TdP”. Moreover, all antiarrhythmic agents except for *dl*-sotalol and amiodarone prolonged TRP to various degrees. Among them, vanoxerine prolonged TRP most potently, indicating that vanoxerine would provide "substrate" for the perpetuation of spiral re-entry more than the others. Thus, agents prolonging J-T_{peak}c more than T_{peak}-T_{end} besides the TRP prolongation in the in vivo QTc model are expected to have a higher risk for inducing TdP.

Tyrosine kinase inhibitors: Imatinib and lapatinib significantly prolonged

JPET Fast Forward. Published on August 21, 2024 as DOI: 10.1124/jpet.124.002184
This article has not been copyedited and formatted. The final version may differ from this version.

QTcV, whereas dasatinib and sunitinib modestly did it (Table 1). Each of the tyrosine kinase inhibitors prolonged J-T_{peak}c to a varying degree without affecting T_{peak}-T_{end}, since they hardly inhibit I_{Kr} in vitro. Dasatinib hardly altered J-T_{peak}c (Table 1) despite prolonging J-T_{peak} itself (+19 ms, not shown in Table 1). While imatinib (+3 bpm), lapatinib (–8 bpm) and sunitinib (+1 bpm) hardly altered the heart rate, dasatinib significantly decreased it by 17 bpm, possibly underestimating the magnitude of its J-T_{peak}c prolongation (Chiba et al, 2022). Onset mechanism of J-T_{peak}c prolongation would deserve a comment along with the involvement of Ca^{2+} dynamics. As tyrosine kinase inhibitors impair mitochondrial function, it can inhibit ATP production, suppress the sarcoplasmic reticulum Ca^{2+}-ATPase as well as sarcolemmal Ca^{2+} pump function and increase intracellular Ca^{2+} concentration, which will enhance the forward-mode Na^{+}-Ca^{2+} exchanger to promote inward current during the plateau phase of action potential, resulting in J-T_{peak}c prolongation (Chiba et al, 2022) (Fig. 5). Thus, imatinib, lapatinib and sunitinib as well as possibly dasatinib may induce early afterdepolarization and ventricular premature beats as a trigger for TdP, but they will not form “substrate” for the initiation of spiral re-entry. However, caution should be paid on the use of tyrosine kinase inhibitors for patients formerly having the spatial dispersion of the ventricle. Imatinib prolonged the TRP most potently among the 4

tyrosine kinase inhibitors, and those 4 tyrosine kinase inhibitors are classified into "possible risk of TdP" in CredibleMeds information (Table 1). In addition, experiments are now ongoing to assess the effects of some other tyrosine kinase inhibitors in our laboratory; for example, nilotinib in a dose of 10 mg/kg/10 min, i.v. showed a similar electrocardiographic profile to those 4 tyrosine kinase inhibitors; namely, a significant prolongation of J-T_{peak}c without affecting T_{peak}-T_{end}, also confirming unique proarrhythmic profile of tyrosine kinase inhibitors.

Antiviral drugs: Each of the antiviral drugs prolonged QTcV, in which T_{peak}-T_{end} was prolonged more potently than J-T_{peak}c, although the effects on TRP vary (Table 1). These findings indicate that the QT-interval prolongation by the antiviral drugs may be largely depend on I_{Kr} inhibition, and that modest J-T_{peak}c prolongation may be associated with additional suppressive action on inward I_{NaL} and I_{CaL}, and enhancement of outward I_{Ks}. Accordingly, the antiviral drugs increase the transmural dispersion of repolarization and some of them may enhance the local electrical vulnerability of ventricles, leading to the formation of substrates for initiating and maintaining the spiral re-entry, respectively. However, they mildly to modestly prolonged J-T_{peak}c, which may indicate a small increase in net inward current during the plateau phase of action potential, suggesting that they will not induce excessive

JPET Fast Forward. Published on August 21, 2024 as DOI: 10.1124/jpet.124.002184
This article has not been copyedited and formatted. The final version may differ from this version.

myocardial Ca^{2+} overload leading to the onset of early afterdepolarization, a trigger for TdP. Thus, since the antiviral drugs will not provide the trigger despite developing the substrates for re-entry, their net potential to develop TdP will be small. However, caution should be paid on the use of antiviral drugs for patients formerly having the trigger for the onset of TdP. Indeed, amantadine is classified into "conditional risk of TdP" in CredibleMeds information, although oseltamivir is done into "low/no risk" in the chronic AV block dogs (Table 1).

Psychotropic drugs: Paliperidone, donepezil and perospirone significantly prolonged QTcV, in which T_{peak}-T_{end} was prolonged more potently than J-T_{peak}c, although the effects on TRP vary (Table 1). Paliperidone is classified into "possible risk of TdP" in CredibleMeds information. Donepezil is classified into "low/no risk" in the chronic AV block dogs but into "known risk of TdP" in CredibleMeds information. No previous information of TdP risk is available for perospirone. On the other hand, lithium modestly prolonged QTcV, and blonanserin and memantine modestly to mildly shortened it, respectively. Lithium is classified into "possible risk of TdP" in CredibleMeds information, whereas no information is available for the TdP risk of blonanserin or memantine.

JPET Fast Forward. Published on August 21, 2024 as DOI: 10.1124/jpet.124.002184
This article has not been copyedited and formatted. The final version may differ from this version.

Antiemetic drugs: Given that several antiemetics are known to prolong QT interval, their systematic evaluation of proarrhythmic surrogate markers of ECG would be important. In a previous clinical study with healthy subjects (Darpo et al., 2020), 2 types of antiemetic 5-HT_3 receptor antagonists ondansetron and dolasetron prolonged QTcF (QT interval corrected with Fridericia's formula) (Fridericia, 2003). Ondansetron, a pure I_{Kr} inhibitor, prolonged J-T_{peak}c with modest T_{peak}-T_{end} prolongation (J-T_{peak}c >T_{peak}-T_{end} pattern). In contrast, dolasetron having mixed ion channel effects (I_{Kr} + I_{Na} inhibition) slightly shortened J-T_{peak}c while prolonging T_{peak}-T_{end} (J-T_{peak}c <T_{peak}-T_{end} pattern). Meanwhile, in our previous study using the in vivo canine QTc model (Satoh et al., 2005), an antiemetic D_2 receptor antagonist prochlorperazine maleate having mixed ion channel effects (I_{Kr} + I_{Na} inhibition) prolonged J-T_{peak}c and T_{peak}-T_{end} to a similar extent (J-T_{peak}c =T_{peak}-T_{end} pattern). Further evaluation is needed since antiemetic agents exert different effects on J-T_{peak}c and T_{peak}-T_{end} depending on the drug.

In silico, in vitro and ex vivo proarrhythmia risk prediction model

The ICH S7B Q&A 4.1 (Anonymous, 2022) states that in silico, in vitro and ex vivo besides in vivo models can be used as part of an integrated risk assessment strategy

to evaluate proarrhythmic risk of QT-interval prolonging pharmaceuticals in humans. A measurable incidence of cardiovascular drugs/compounds- and non-cardiovascular drugs-induced TdP/risk by in silico, in vitro and ex vivo proarrhythmia models is summarized in Tables 4 left and 5 left, respectively. Among them, the use of in silico and in vitro models may have a certain advantage in reducing animal use by the 3Rs (reduce/refine/replace).

CiPA in silico model: The electrophysiological effects of drugs/compounds on 4 types of human myocardial ionic currents including I_{Kr}, I_{Na}, I_{NaL} and I_{CaL} are evaluated by the voltage clamp method (Sager et al., 2014). The results are used to quantify the proarrhythmic risk of drugs/compounds by reconstructing action potentials in an in silico cardiomyocyte model. A proarrhythmic score is calculated, which is confirmed by a multichannel assay system, such as induced pluripotent stem (iPS) cell-derived cardiomyocytes. When the development of a candidate compound is to proceed, in vivo/clinical ECG studies will be conducted to confirm that no unexpected changes occur in the PR interval, QRS width, QT interval, heart rate or QT waveform. An analysis of 12 training and 16 validation agents evaluated in compliance with S7B Q&As was reported in 2019 (Li et al., 2019). However, the CiPA in silico model by itself was designed to integrate the risk of instability of repolarization processes that

may cause TdP, which is not a model to directly detect drug-induced TdP. Importantly, the effects of pharmacokinetics and autonomic innervation on cardiac electrophysiology have not been considered with this model, so caution should be exercised when extrapolating the results obtained to humans. Meanwhile, another group devised a novel methodology to overcome some of these challenges (Llopis-Lorente et al., 2023). The proposed methodology combines pharmacokinetic and electrophysiological models to incorporate the effects of sex and renal function into in silico drug simulations, which may improve and accelerate the prediction of drug-induced TdP risks.

iPS cell-derived cardiomyocyte sheet model: This model detects the drug-induced repolarization delay by recording the action potentials or field potentials of human iPS cell-derived cardiomyocytes as indicators. By conducting evaluations of the electrophysiological effects of numerous compounds, the application of this model to safety pharmacology studies was vigorously pursued by several research teams (Nakamura et al., 2014; Matsuo et al., 2015; Yamamoto et al., 2016; Ando et al., 2017; Izumi-Nakaseko et al., 2017a, 2017c, 2018, 2020ab, 2023a; Sugiyama et al., 2019; Altrocchi et al., 2020). This model can also detect early afterdepolarization and triggered activity derived from drug-induced repolarization delay, which can be used for follow-up study as described in S7B Q&As 2.2-2.5.

JPET Fast Forward. Published on August 21, 2024 as DOI: 10.1124/jpet.124.002184
This article has not been copyedited and formatted. The final version may differ from this version.

Langendorff-perfused isolated heart preparation: The Langendorff-perfused heart model allows the evaluation of drug-induced proarrhythmic effects while preserving the electrical and physical properties of the whole heart (Kannankeril et al., 2010). Rabbit or guinea pig hearts are often used. In some cases, the His bundle is cut and the ventricles are electrically paced (Eckardt et al., 1998). The model is often used to assess the spatial and temporal variability of the repolarization process (Hondeghem et al., 2001). It can detect TdP and has been used to evaluate a great number of drugs as a proarrhythmia model (Hondeghem et al., 2001).

Arterially-perfused, ventricular wedge preparation: The left ventricle of dogs or rabbits is isolated and perfused with the physiological nutrient solution through the anterior descending branch of the left coronary artery (Liu et al., 2006; Kannankeril et al., 2010). Electrodes are placed across the left ventricular free wall to record ECG, whereas action potentials are obtained from 3 distinct cell types (endocardial, M cells and epicardial) using floating electrodes to directly evaluate spatial variability in the repolarization process (Shimizu et al., 1997). Arrhythmias can be detected by using the failing myocardium of dogs (Akar et al., 2003), but the model has been rarely used for detecting drug-induced arrhythmias.

Blood-perfused, ventricular muscle preparation: The ventricular septum of

JPET Fast Forward. Published on August 21, 2024 as DOI: 10.1124/jpet.124.002184
This article has not been copyedited and formatted. The final version may differ from this version.

a beagle dog is excised, a blood perfusion cannula is inserted into the anterior septal artery, and a stimulating electrode is sewn onto the His-bundle region (Sugiyama et al., 1994). After cross-circulated with arterial blood from a halothane-anesthetized dog, monophasic action potentials are recorded from the base of the right ventricular papillary muscle (Sugiyama and Hashimoto, 2002). TdP is reproducibly elicited when an extra-stimulus is applied to phase 3 of the action potential while an I_{Kr} inhibitor is continuously administered into the nutrient coronary artery of the preparation. Although it has excellent sensitivity and specificity for detecting the drug-induced TdP, its technical difficulty limits the number of facilities where it can be performed.

In vivo proarrhythmia risk prediction model

The in silico and in vitro models as well as in vivo proarrhythmia models are useful for studying "non-double negative" compounds in the follow-up study (Strauss et al., 2021; Rossman et al., 2023). Importantly, in vivo models can evaluate the proarrhythmic effects of drugs in the presence of metabolic, hormonal and neural influences. Since the pathways of drug metabolism in some animals may differ from those in humans, caution may be required in interpreting the results (Sugiyama, 2008; Goto et al., 2020a, 2021, 2022). To date, chronic AV block models have been

developed using dogs, monkeys, rabbits and pigs, whereas ready-to-use in vivo models and genetically engineered animal models are also available. A measurable incidence of cardiovascular drugs/compounds- and non-cardiovascular drugs-induced TdP/risk by those in vivo proarrhythmia models is summarized in Tables 4 right and 5 right, respectively. Recently, several useful proarrhythmia models of rabbits have been created.

Chronic AV block canine model: This model has high sensitivity and specificity to detect the drug-induced TdP, and has been used for safety evaluation of new drug candidate compounds. An excellent review article on the chronic AV block canine model was published by a group in the Netherlands (Loen et al., 2022), and interested readers are referred to it. A beagle dog is put under general anesthesia with thiopental sodium, tip of the electrode catheter is placed on the AV nodal region, and radiofrequency waves are applied from the tip to destroy the AV node, creating a complete AV block with a stable ventricular escaped rhythm (Sugiyama et al., 2002ab; Sugiyama, 2008). To compensate for the bradycardia-associated heart failure, various neurohumoral factors are secreted and the myocardial remodeling proceeds. The resulting reduction in repolarization reserve is the basis for the development of drug-induced long QT syndrome (Fig. 4). In the "canine" model, drug-induced TdP

JPET Fast Forward. Published on August 21, 2024 as DOI: 10.1124/jpet.124.002184
This article has not been copyedited and formatted. The final version may differ from this version.

can be detected within 4 weeks after the creation of a complete AV block. The model can evaluate the TdP risk of a drug/compound both under anesthesia and conscious state. We discussed the risk stratification of QT-prolonging drugs/compounds in the next paragraph primarily based on our previous publications obtained by the conscious AV block canine model.

The results of risk stratification for cardiovascular agents and non-cardiovascular drugs at doses less than and greater than 3 times the maximum clinical daily dose assessed in the conscious chronic AV block dogs are summarized in Table 2. Drugs that induce TdP at ≤3 times the maximum clinical daily dose reflecting clinically-relevant exposure can be classified as "high risk" drugs; those do not induce TdP at ≤3 times the maximum clinical daily dose but do induce TdP at higher doses (>3 times) are classified as "intermediate risk"; and those that do not induce TdP at all are classified as "low/no risk". In the case of the chronic AV block "canine" model, most of the animals experiencing TdP exert ventricular fibrillation and die, so direct comparisons of positive control drugs with new drug candidate compounds or dose-response evaluations of drug candidates cannot be conducted using the same animals.

Chronic AV block monkey model: A chronic AV block "monkey" model can

JPET Fast Forward. Published on August 21, 2024 as DOI: 10.1124/jpet.124.002184
This article has not been copyedited and formatted. The final version may differ from this version.

be created in cynomolgus monkeys using the same technique as that in the "canine" model (Sugiyama et al., 2002ab; Sugiyama, 2008; Goto et al., 2021; Izumi-Nakaseko et al., 2023b). In the "monkey" model, drug-induced TdP can be detected normally within 7 months after the creation of a complete AV block. As in the "canine" model, the risk of drug-induced TdP can be assessed by "monkey" model under anesthesia and conscious state. The results of risk stratification for antiarrhythmic agents and non-cardiovascular drugs at doses less than and greater than 3 times the maximum clinical daily dose assessed in the conscious chronic AV block monkeys are summarized in Table 3. The "monkey" model has a similar sensitivity and specificity to detect TdP as the "canine" model, when the drug metabolic pathways are close between the monkeys and dogs (Tables 2 and 3). However, it should be noted that dogs do not express CYP3A4 or its alternative enzymes, whereas cynomolgus monkeys do not have CYP3A4 either but express CYP3A8 which functions like human CYP3A4. Thus, the plasma concentration of drugs like terfenadine, cisapride, astemizole and haloperidol that are metabolized by CYP3A4 may become higher in dogs than in monkeys, thus making the occurrence of TdP greater in dogs except for astemizole (Tables 2 and 3) (Goto et al., 2020a, 2021, 2022). Since astemizole itself and its metabolite desmethylastemizole can inhibit I_{Kr} with a similar potency and sum of the blood

concentrations of both was higher in monkeys than in dogs after 10 mg/kg, p.o., TdP was induced by lower dose of astemizole in monkeys than in dogs (Izumi-Nakaseko et al., 2016; Goto et al., 2022). Moreover, the TdP developed in the "monkey" model largely terminated spontaneously unlike in the "canine" model, allowing multiple-drug comparisons and dose-response assessments to be performed using the same animals. Repeated use can greatly reduce the number of animals needed for experiments (3Rs) (Goto et al., 2020ab).

Chronic AV block pig model: It has been reported that AV block can be induced in the ultra-compact laboratory miniature pig (*microminipig*) by catheter ablation under closed chest conditions as in dogs and monkeys (Kaneko et al., 2011; Sugiyama et al., 2011). Administration of I_{Kr} inhibitors prolonged QT interval greater in “pig” model than in “canine” and “monkey” models, but TdP was not induced in “pig” model” unlike in the others (Sugiyama et al., 2011; Goto et al., 2019a; 2020a). One reason for this is that, unlike other animal models, in the "pig" model, I_{Kr} inhibitors hardly prolonged the early repolarization period (Yokoyama et al., 2017; Goto et al., 2019b). Similarly, Langendorff-perfused Göttingen minipig hearts are shown to be resistant to the development of ventricular arrhythmias in experimental settings known to be proarrhythmic in other species including dogs due to a very small STV in the

JPET Fast Forward. Published on August 21, 2024 as DOI: 10.1124/jpet.124.002184
This article has not been copyedited and formatted. The final version may differ from this version.

action potential duration (Laursen et al., 2011).

Chronic AV block rabbit model: Formaldehyde solution is injected into the AV junctional area under an open chest to create AV block. A pacemaker for ventricular stimulation is implanted, and after the chest is closed, the ventricle is paced at 180-200 beats/min for 5 days postoperatively. Subsequently, during 6 weeks of observation period under escaped ventricular rhythm, animals showed a marked QT-interval prolongation and spontaneous TdP episodes (27/34 cases; 71%) (Tsuji et al., 2002). The "rabbit" model is characterized by repeated spontaneous TdP episodes. In ventricular myocytes isolated from rabbits with chronic AV block, an approximately 50% reduction in K^+ channel (I_{Kr} and I_{Ks}) current density and a voltage-dependent hyperpolarizing shift of L-type Ca^{2+} channels were observed, and such electrical remodeling has been implicated for the proarrhythmic events (Tsuji et al., 2002). It is also possible to destroy the AV node by catheter ablation under closed chest conditions as in dogs and monkeys (Hagiwara et al., 2015). Among the group of 23 rabbits that underwent AV block induction by catheter ablation, 14 showed a stable condition in rhythm and hemodynamics for 2-5 h after the procedure. Despite initially stable conditions, 2 rabbits did not survive within the first two days afterward. By the 4 weeks, 7 rabbits passed away, likely due to developing TdP. This inference is based on

JPET Fast Forward. Published on August 21, 2024 as DOI: 10.1124/jpet.124.002184
This article has not been copyedited and formatted. The final version may differ from this version.

the absence of abnormal physical signs during their recovery and the demonstration of TdP occurrence with a Holter ECG in one of them. Interestingly, 5 rabbits surpassed expectations, surviving beyond 4 weeks, resulting in a 22% survival rate (Hagiwara et al., 2015). Although this model has not been used to evaluate the safety of new drug candidate compounds, it can be applied to study the mechanism of ventricular arrhythmias with repolarization abnormalities and the treatment of lethal arrhythmias (Tsuji et al., 2011; Hagiwara et al., 2015).

Acute AV block rabbit model: This is a closed chest model created by anesthetizing normal rabbits with ketamine and xylazine followed by inhalation of isoflurane, and catheter ablation to destroy the AV node (Hagiwara et al., 2015, 2016, 2017). A testing drug is administered intravenously to assess its proarrhythmic effects, while the ventricles are electrically driven at 60 beats/min through an electrode catheter placed in the right ventricle. Dofetilide, nifekalant, sparfloxacin and haloperidol, which are clinically known to prolong QT interval and induce TdP, developed TdP spontaneously in this model, whereas amiodarone and moxifloxacin, which are known to prolong QT interval but rarely to induce TdP, did not develop TdP (Hagiwara et al., 2015, 2017). This model is more sensitive to detect TdP than Carlsson model as discussed below (Hagiwara et al., 2017), and also allows evaluation of the

proarrhythmic effects of drugs with α_1-adrenoceptor blocking action such as antipsychotic medications and antihistamines (Hagiwara et al., 2016; Kawakami et al., 2020). Ventricular muscle removed from normal rabbits was more proarrhythmic than that from dogs with chronic AV block (Nakaya et al., 1993; Takahara et al., 2007). In addition, these electrophysiological properties of rabbit ventricular muscle were more likely to be manifested at lower heart rates (60 bpm) than under sinus rhythm (200-250 bpm) in vivo (Hagiwara et al., 2017). These findings are explained by a cellular electrophysiological property specific to rabbit ventricular muscle, in which the density of I_{Ks} is small (Lu et al., 2001; Hagiwara et al., 2017). Isoflurane, used as an anesthetic in this model, promotes Ca^{2+}-induced Ca^{2+} release from the sarcoplasmic reticulum (Akata et al., 2001), and xylazine is known to inhibit sympathetic nerve activity via adrenergic α_2-receptor stimulation (Allen et al., 1988), suggesting that those medications may also be associated with the sensitivity of this model.

Methoxamine-sensitized rabbit model (Carlsson Model): Normal rabbits are anesthetized with thiopental and maintained with α-chloralose while receiving continuous intravenous dosing of α_1-adrenoceptor agonist methoxamine. A testing drug is administered continuously for 30 min from 10 min after the start of methoxamine infusion to evaluate its proarrhythmic effects (Carlsson et al., 1993).

JPET Fast Forward. Published on August 21, 2024 as DOI: 10.1124/jpet.124.002184
This article has not been copyedited and formatted. The final version may differ from this version.

Advantages include the simplicity and low cost of experimental manipulation. Challenges include the low sensitivity in detecting TdP, the need to consider drug interactions with methoxamine even when TdP is induced, the high possibility of false negative results especially with drugs that have α_1-adrenoceptor blocking effect, and the fact that evaluation is limited to intravenous administration under anesthesia, making prolonged studies and repeated drug administration difficult. It had been postulated in this model that the direct effects of α_1-adrenoceptor stimulation on the myocardium might be responsible for arrhythmogenesis. However, a study showed that the proarrhythmic effects of class III antiarrhythmic drug clofilium became undetectable after surgical excision of bilateral vagal nerves, indicating that vagal bradycardia produced as a reflex to pressure elevation by α_1-adrenoceptor stimulation is strongly involved in the onset of drug-induced TdP (Farkas et al., 2008).

Genetically engineered rabbit models: LQT1, 2, 5, 6, 7, 11 and 13 are known as types of long QT syndromes in which outward K^+ current is reduced. Among them, LQT1, 2 and 5 gene-modified rabbits were developed, and their cardiac electrophysiological characteristics have been investigated. LQT1 rabbits were generated by introducing the Y315S mutation into KCNQ1, the gene for the α subunit (KvLQT1) that forms the I_{Ks} channel pore, whereas LQT2 rabbits were created by

JPET Fast Forward. Published on August 21, 2024 as DOI: 10.1124/jpet.124.002184
This article has not been copyedited and formatted. The final version may differ from this version.

introducing the G628S mutation into KCNH2, the gene for the α subunit (ERG) that forms the I_{Kr} channel pore (Brunner et al., 2008). Each genetically modified rabbit shows marked reductions in respective targeted I_{Ks} and I_{Kr}, and QT interval is prolonged by approximately 30% in LQT1 rabbits and 50% in LQT2 rabbits compared to healthy animals. LQT1 rabbits show no signs of lethal arrhythmias, whereas sudden death due to spontaneous onset of TdP has been observed in LQT2 rabbits with a reported survival rate of approximately 50% at 1 year. In addition to a marked reduction in each targeted I_{Ks} and I_{Kr} current, I_{Kr} is reduced to approximately 2/3 in LQT1 rabbits and I_{Ks} to approximately 3/4 in LQT2 rabbits, but no change is observed in I_{to} or I_{K1}. In a subsequent study, LQT5 rabbits were generated by introducing the G52R mutation into KCNE1, the gene for the β-subunit (minK) of I_{Ks} channel. LQT5 rabbits showed no difference from wild-type animals in QT interval, and their current amplitudes of I_{Ks} and I_{Kr} channels were comparable to those of wild-type animals (Major et al., 2016). LQT5 rabbits were experimentally shown to be more sensitive to class III antiarrhythmic drug dofetilide, indicating that an enhanced deactivation rate of I_{Ks} and I_{Kr} channels may be involved in this mechanism. Based on these electrophysiological characteristics, LQT5 rabbit is positioned as a silent LQT model with a reduced repolarization reserve. Thus, the characteristics of genetically modified rabbits differ

among LQT types, and the LQT1 or LQT5 model is recommended for the safety evaluation of new drug candidate compounds, whereas the LQT2 model is expected to be applied as a mechanistic study of sudden cardiac death. Although studies on drug-induced arrhythmias have focused on those compounds that inhibit I_{Kr} channels, drugs that inhibit I_{K1} or I_{Ks} channels are also thought to have arrhythmogenic risks. A recent study reported that the LQT2 plus LQT5 model having mutations in their respective genes can be used to study proarrhythmic effects of drugs that inhibit I_{K1} and I_{Ks} channels (Hornyik et al., 2020).

Study limitation and clinical application

Most of the TdP risk scores reported in the chronic AV block dogs and monkeys, and the CredibleMeds are qualitatively and quantitatively in accordance with the changes in the in vivo proarrhythmic surrogate markers including the QTcV, J-T_{peak}c, T_{peak}-T_{end} and TRP, although some discrepancies exist among them (Table 1). Supplementing the information on drugs, for which the TdP risk has not yet been assessed using the chronic AV block dogs or monkeys, would further confirm the sensitivity and reliability of those surrogate markers. Since those concepts of surrogate markers are established in normal animals and healthy human subjects, the

JPET Fast Forward. Published on August 21, 2024 as DOI: 10.1124/jpet.124.002184
This article has not been copyedited and formatted. The final version may differ from this version.

time courses of changes in those surrogate markers before the onset of TdP should be verified using the proarrhythmia models as well as in patients. We assume that even when TdP eventually occurs in such pathologically modified hearts, there may be diversity in its onset mode, including trigger-dominant type (J-T_{peak}c >T_{peak}-T_{end} pattern; high frequency of extrasystoles occasionally causing TdP), substrate-dominant type (J-T_{peak}c <T_{peak}-T_{end} pattern; low frequency of extrasystoles normally causing TdP) and their intermediate type (J-T_{peak}c =T_{peak}-T_{end} pattern; moderate frequency of extrasystoles sometimes causing TdP).

Conclusion

This review detailed the onset mechanisms of drug-induced TdP, including I_{Kr} inhibition, pharmacokinetic factors, autonomic regulation and reduced repolarization reserve. It also explored the utility of proarrhythmic surrogate markers (J-T_{peak}, T_{peak}-T_{end} and TRP) besides QT interval. Finally, it presented various in silico, in vitro, ex vivo and in vivo models for proarrhythmic risk prediction (Tables 4 and 5). For most of the drugs, the results of risk assessment are the same among the models. However, for a small number of drugs, there are models, in which drugs classified as 'high risk' in the chronic AV block dog assessment did not induce TdP in other model,

and conversely, those classified as 'low/no risk' did induce arrhythmia in other one. Such differences in risk assessment among the models reflect the characteristics of each model, including pharmacokinetic factors and/or autonomic regulation. Thus, those proarrhythmia models along with the surrogate markers can play important roles in quantifying TdP risk of new compounds, impacting late-phase clinical design and regulatory decision-making, and preventing adverse events on post-marketing clinical use.

JPET Fast Forward. Published on August 21, 2024 as DOI: 10.1124/jpet.124.002184
This article has not been copyedited and formatted. The final version may differ from this version.

Acknowledgments

The authors thank Dr. Yuko Sekino, Dr. Yasunari Kanda, Dr. Kohei Sawada and Dr. Takashi Yoshinaga for their scientific advice to establish iPS-cell derived cardiomyocyte sheet model; Dr. Yuji Nakamura (deceased on March 26, 2018), Dr. Xin Cao, Dr. Koki Chiba, Dr. Katsuyoshi Chiba, Dr. Mihoko Hagiwara-Nagasawa, Dr. Takeshi Wada, Dr. Yoshio Nunoi, Dr. Suchitora Matsukura, Dr. Kentaro Ando, Dr. Yasuki Akie, Dr. Yoshioki Satoh, Dr. Katsuhiko Itoh and Mr. Kengo Sakamoto for their great contribution to develop chronic AV block proarrhythmia animal models; and Mrs. Yuri Ichikawa, Ms. Misako Saito and Mr. Makoto Shinozaki for their technical assistance.

Data Availability Statement

There are no datasets in my paper.

Authorship Contributions

Participated in research design: Sugiyama

Performed data analysis: Sugiyama, Goto, and Kambayashi

Wrote or contributed to the writing of the manuscript: Sugiyama, Goto, Izumi-Nakaseko, Takei, Takahara, and Kambayashi

References

Akar FG and Rosenbaum DS (2003) Transmural electrophysiological heterogeneities underlying arrhythmogenesis in heart failure. Circ Res 93: 638-645.

Akata T, Nakashima M, and Izumi K (2001) Comparison of volatile anesthetic actions on intracellular calcium stores of vascular smooth muscle: investigation in isolated systemic resistance arteries. Anesthesiology 94: 840-850.

Akita M, Shibazaki Y, Izumi M, Hiratsuka K, Sakai T, Kurosawa T, and Shindo Y (2004) Comparative assessment of prurifloxacin, sparfloxacin, gatifloxacin and levofloxacin in the rabbit model of proarrhythmia. J Toxicol Sci 29: 63-71.

Allen JM, McCarron JG, McHale NG, and Thornbury KD (1988) Release of [^{3}H]-noradrenaline from the sympathetic nerves to bovine mesenteric lymphatic vessels and its modification by α-agonists and antagonists. Br J Pharmacol 94: 823-833.

Altrocchi C, de Korte T, Bernardi J, Spätjens RLHMG, Braam SR, Heijman J, Zaza A, and Volders PGA (2020) Repolarization instability and arrhythmia by I_{Kr} block in single human-induced pluripotent stem cell-derived cardiomyocytes and 2D monolayers. Europace 22: 1431-1441.

Anderson ME, Mazur A, Yang T, and Roden DM (2001) Potassium current antagonist properties and proarrhythmic consequences of quinolone antibiotics. J Pharmacol Exp Ther 296: 806-810.

Ando H, Yoshinaga T, Yamamoto W, Asakura K, Uda T, Taniguchi T, Ojima A, Shinkyo R, Kikuchi K, Osada T, Hayashi S, Kasai C, Miyamoto N, Tashibu H, Yamazaki D, Sugiyama A, Kanda Y, Sawada K, and Sekino Y (2017) A new paradigm for drug-induced torsadogenic risk assessment using human iPS cell-derived cardiomyocytes. J Pharmacol Toxicol Methods 84: 111-127.

Ando K, Wada T, and Cao X (2020) Precise safety pharmacology studies of lapatinib for onco-cardiology assessed using in vivo canine models. Sci Rep 10: 738.

Anonymous (2005a) ICH steering committee, the non-clinical evaluation of the potential for delayed ventricular repolarization (QT interval prolongation) by human pharmaceuticals (S7B). The Guideline was recommended for adoption at Step 4 of the ICH process on May 12, 2005, Accessed February 12, 2024, https://www.pmda.go.jp/files/000156513.pdf.

Anonymous (2005b) ICH steering committee, the clinical evaluation of QT/QTc interval prolongation and proarrhythmic potential for non-antiarrhythmic drugs (E14). The Guideline was recommended for adoption at Step 4 of the ICH

process on May 12, 2005, Accessed February 12, 2024, https://www.pmda.go.jp/files/000156582.pdf.

Anonymous (2022) ICH E14/S7B implementation working group, clinical and nonclinical evaluation of QT/QTc interval prolongation and proarrhythmic potential questions and answers. The Q&As were recommended for adoption at Step 4 of the ICH process on February 21, 2022, Accessed February 12, 2024, https://www.pmda.go.jp/files/000247627.pdf .

Asano Y, Davidenko JM, Baxter WT, Gray RA, and Jalife J (1997) Optical mapping of drug-induced polymorphic arrhythmias and torsade de pointes in the isolated rabbit heart. J Am Coll Cardiol 29: 831-842.

Batey AJ, and Coker SJ (2002) Proarrhythmic potential of halofantrine, terfenadine, and clofilium in a modified in vivo model of torsade de pointes. Br J Pharmacol 135: 1003-1012.

Bourgonje VJ, Vos MA, Ozdemir S, Doisne N, Acsai K, Varro A, Sztojkov-Ivanov A, Zupko I, Rauch E, Kattner L, Bito V, Houtman M, van der Nagel R, Beekman JD, van Veen TA, Sipido KR, and Antoons G (2013) Combined Na^+/Ca^{2+} exchanger and L-type calcium channel block as a potential strategy to suppress arrhythmias and maintain ventricular function. Circ Arrhythm Electrophysiol 6:

371-379.

Brunner M, Peng X, Liu GX, Ren XQ, Ziv O, Choi BR, Mathur R, Hajjiri M, Odening KE, Steinberg E, Folco EJ, Pringa E, Centracchio J, Macharzina RR, Donahay T, Schofield L, Rana N, Kirk M, Mitchell GF, Poppas A, Zehender M, and Koren G (2008) Mechanisms of cardiac arrhythmias and sudden death in transgenic rabbits with long QT syndrome. J Clin Invest 118: 2246-2259.

Buchanan LV, Kabell G, Brunden MN, and Gibson JK (1993) Comparative assessment of ibutilide, D-sotalol, clofilium, E-4031, and UK-68,798 in a rabbit model of proarrhythmia. J Cardiovasc Pharmacol 22: 540-549.

Cao X, Nakamura Y, Wada T, Izumi-Nakaseko H, Ando K, and Sugiyama A (2016) Electropharmacological effects of amantadine on cardiovascular system assessed with J-T_{peak} and T_{peak}-T_{end} analysis in the halothane-anesthetized beagle dogs. J Toxicol Sci 41: 439-447.

Cao X, Nakamura Y, Wada T, Izumi-Nakaseko H, Ando K, and Sugiyama A (2017) L/N-type Ca^{2+} channels blocker cilnidipine ameliorated the repolarization abnormality in a chronic hemodialysis patient. Heart Vessels 32: 105-108.

Carlsson L, Almgren O, and Duker G (1990) QTU-prolongation and torsades de pointes induced by putative class III antiarrhythmic agents in the rabbit. J Cardiovasc

Pharmacol 16: 276-285.

Carlsson L, Abrahamsson C, Andersson B, Duker G, and Schiller-Linhardt G (1993) Proarrhythmic effects of the class III antiarrhythmic agent almokalant– importance of rate of infusion, QT interval dispersion and early afterdepolarizations. Cardiovasc Res 27: 2186-2193.

Carlsson L, Amos GJ, Andersson B, Drews L, Duker G, and Wadstedt G (1997) Electrophysiological characterization of the prokinetic agents cisapride and mosapride in vivo and in vitro: implications for pro-arrhythmic potential? J Pharmacol Exp Ther 282: 220-227.

Chen X, Cass JD, Bradley JA, Dahm CM, Sun Z, Kadyszewski E, Engwall MJ, and Zhou J (2005) QT prolongation and proarrhythmia by moxifloxacin: concordance of preclinical models in relation to clinical outcome. Br J Pharmacol 146: 792-799.

Chiba K, Sugiyama A, Satoh Y, Shiina H, and Hashimoto K (2000) Proarrhythmic effects of fluoroquinolone antibacterial agents: In vivo effects as physiologic substrate for torsades. Toxicol Appl Pharmacol 169: 8-16.

Chiba K, Sugiyama A, Hagiwara T, Takahashi S, Takasuna K, and Hashimoto K (2004) In vivo experimental approach for the risk assessment of fluoroquinolone

antibacterial agents-induced long QT syndrome. Eur J Pharmacol 486: 189-200.

Chiba K, Wada T, Nakamura Y, Cao X, Hagiwara-Nagasawa M, Izumi-Nakaseko H, Ando K, Tanaka K, Naito AT, and Sugiyama A (2017) Analysis of proarrhythmic potential of an atypical antipsychotic drug paliperidone in the halothane-anesthetized dogs. J Pharmacol Sci 134: 239-246.

Chiba K, Kambayashi R, Onozato M, Goto A, Izumi-Nakaseko H, Takei Y, Matsumoto A, Tanaka K, Kanda Y, Fukushima T, and Sugiyama A (2022) Imatinib induces diastolic dysfunction and ventricular early-repolarization delay in the halothane-anesthetized dogs: Class effects of tyrosine kinase inhibitors. J Pharmacol Sci 150: 154-162.

Chui RW, Baublits J, Chandra FA, Jones ZW, Engwall MJ, and Vargas HM (2021) Evaluation of moxifloxacin in canine and non-human primate telemetry assays: Comparison of QTc interval prolongation by timepoint and concentration-QTc analysis. Clin Transl Sci 14: 2379–2390.

Darpo B, Sarapa N, Garnett C, Benson C, Dota C, Ferber G, Jarugula V, Johannesen L, Keirns J, Krudys K, Ortemann-Renon C, Riley S, Rogers-Subramaniam D, and Stockbridge N (2014) The IQ-CSRC prospective clinical Phase 1 study: “Can

early QT assessment using exposure response analysis replace the thorough QT study?". Ann Noninvasive Electrocardiol 19: 70-81.

Darpo B, Benson C, Brown R, Dota C, Ferber G, Ferry J, Jarugula V, Keirns J, Ortemann-Renon C, Pham T, Riley S, Sarapa N, Ticktin M, Zareba W, and Couderc JP (2020) Evaluation of the Effect of 5 QT-Positive Drugs on the JTpeak Interval - An Analysis of ECGs From the IQ-CSRC Study. J Clin Pharmacol 60: 125-139.

Delaunois A, Abernathy M, Anderson WD, Beattie KA, Chaudhary KW, Coulot J, Gryshkova V, Hebeisen S, Holbrook M, Kramer J, Kuryshev Y, Leishman D, Lushbough I, Passini E, Redfern WS, Rodriguez B, Rossman EI, Trovato C, Wu C, and Valentin JP (2021) Applying the CiPA approach to evaluate cardiac proarrhythmia risk of some antimalarials used off-label in the first wave of COVID-19. Clin Transl Sci 14: 1133-1146.

Di Diego JM, Belardinelli L, and Antzelevitch C (2003) Cisapride-induced transmural dispersion of repolarization and torsade de pointes in the canine left ventricular wedge preparation during epicardial stimulation. Circulation 108: 1027-1033.

Eckardt L, Haverkamp W, Mertens H, Johna R, Clague JR, Borggrefe M, and Breithardt G (1998) Drug-related torsades de pointes in the isolated rabbit heart:

comparison of clofilium, *d,l*-sotalol, and erythromycin. J Cardiovasc Pharmacol 32: 425-434.

Ellermann C, Coenen A, Niehues P, Leitz P, Kochhäuser S, Dechering DG, Fehr M, Eckardt L, and Frommeyer G (2020) Proarrhythmic effect of acetylcholine-esterase inhibitors used in the treatment of Alzheimer's disease: benefit of rivastigmine in an experimental whole-heart model. Cardiovasc Toxicol 20: 168-175.

Farkas A, Dempster J, and Coker SJ (2008) Importance of vagally mediated bradycardia for the induction of torsade de pointes in an in vivo model. Br J Pharmacol 154: 958-970.

Fridericia LS (2003) The duration of systole in an electrocardiogram in normal humans and in patients with heart disease. Ann Noninvasive Electrocardiol 8: 343-351.

Goto A, Izumi-Nakaseko H, Hagiwara-Nagasawa M, Chiba K, Ando K, Naito AT, and Sugiyama A (2018a) Analysis of torsadogenic and pharmacokinetic profile of E-4031 in dogs bridging the gap of information between in vitro proarrhythmia assay and clinical observation in human subjects. J Pharmacol Sci 137: 237-240.

Goto A, Nakamura Y, Lubna NJ, Chiba K, Hagiwara-Nagasawa M, Izumi-Nakaseko H,

Ando K, Naito AT, and Sugiyama A (2018b) Analysis of safety margin of lithium carbonate against cardiovascular adverse events assessed in the halothane-anesthetized dogs. Cardiovasc Toxicol 18: 530-536.

Goto A, Hagiwara-Nagasawa M, Chiba K, Kambayashi R, Nunoi Y, Izumi-Nakaseko H, Matsumoto A, Kanda Y, and Sugiyama A (2019a) Pharmacological β-adrenoceptor blockade can augment torsadogenic action of I_{Kr} inhibitor: Comparison of proarrhythmic effects of *d*-sotalol and *dl*-sotalol in the chronic atrioventricular block dogs. J Pharmacol Sci 141; 86-89.

Goto A, Hagiwara-Nagasawa M, Kambayashi R, Chiba K, Izumi-Nakaseko H, Naito AT, Kanda Y, and Sugiyama A (2019b) Measurement of J-T_{peak}c along with QT-interval prolongation may increase the assay sensitivity and specificity for predicting the onset of drug-induced torsade de pointes: Experimental evidences based on proarrhythmia model animals. Cardiovasc Toxicol 19: 357-364.

Goto A, Sakamoto K, Hagiwara-Nagasawa M, Kambayashi R, Chiba K, Nunoi Y, Izumi-Nakaseko H, Matsumoto A, and Sugiyama A (2020a) Utilization of the chronic atrioventricular block cynomolgus monkey as an in vivo model to evaluate drug interaction-associated torsade de pointes. J Pharmacol Sci 142:

172-175.

Goto A, Sakamoto K, Hagiwara-Nagasawa M, Kambayashi R, Chiba K, Nunoi Y, Izumi-Nakaseko H, Takei Y, Matsumoto A, and Sugiyama A (2020b) In vivo analysis of the effects of intravenously as well as orally administered moxifloxacin on the pharmacokinetic and electrocardiographic variables along with its torsadogenic action in the chronic atrioventricular block monkeys. J Pharmacol Sci 143: 272-280.

Goto A, Sakamoto K, Kambayashi R, Nunoi Y, Izumi-Nakaseko H, Kawai S, Takei Y, Matsumoto A, Kanda Y, and Sugiyama A (2021) Torsadogenic action of cisapride, *dl*-sotalol, bepridil and verapamil analyzed by the chronic atrioventricular block cynomolgus monkeys: Comparison with that reported in the CiPA in silico mechanistic model. Toxicol Sci 181: 125-133.

Goto A, Sakamoto K, Kambayashi R, Izumi-Nakaseko H, Kawai S, Takei T, Matsumoto A, Kanda Y, and Sugiyama A (2022) Validation of risk-stratification method for the chronic atrioventricular block cynomolgus monkey model and its mechanistic interpretation using 6 drugs with pharmacologically-distinct profile. Toxicol Sci 190: 99-109.

Goto A, Kambayashi R, Izumi-Nakaseko H, Shinozaki M, Takei Y, and Sugiyama A

(2023) Characterization of electropharmacological profile of an anti-atrial fibrillatory drug vernakalant along with potential risk toward torsade de pointes: Translational studies using isoflurane-anesthetized dogs and isolated rat aortic preparations. J Pharmacol Sci 152: 201-209.

Gotta, V, Cools F, van Ammel K, Gallacher DJ, Visser SA, Sannajust F, Morissette P, Danhof M, and van der Graaf PH (2015) Sensitivity of pharmacokinetic-pharmacodynamic analysis for detecting small magnitudes of QTc prolongation in preclinical safety testing. J Pharmacol Toxicol Methods 72: 1-10.

Guérard NC, Traebert M, Suter W, and Dumotier BM (2008) Selective block of I_{Ks} plays a significant role in MAP triangulation induced by I_{Kr} block in isolated rabbit heart. J Pharmacol Toxicol Methods 58: 32-40.

Hagiwara M, Kondo N, Chiba T, and Takahara A (2015) Proarrhythmic properties of the atrioventricular block heart of the rabbit. Jpn. J. Electrophysiology 35: 169-176 (In Japanese with English abstract).

Hagiwara M, Kambayashi R, Aimoto M, Nagasawa Y, and Takahara A (2016) In vivo analysis of torsadogenic potential of an antipsychotic drug paliperidone using the acute atrioventricular block rabbit as a proarrhythmia model. J Pharmacol

Sci 132: 48-54.

Hagiwara M, Shibuta S, Takada K, Kambayashi R, Nakajo M, Aimoto M, Nagasawa Y, and Takahara A (2017) The anaesthetized rabbit with acute atrioventricular block provides a new model for detecting drug-induced torsade de pointes. Br J Pharmacol 174: 2591-2605.

Hagiwara-Nagasawa M, Kambayashi R, Goto A, Nunoi Y, Izumi-Nakaseko H, Takei Y, Matsumoto A, and Sugiyama A (2021a) Cardiohemodynamic and arrhythmogenic effects of the anti-atrial fibrillatory compound vanoxerine in halothane-anesthetized dogs. Cardiovasc Toxicol 20:419-426

Hagiwara-Nagasawa M, Kambayashi R, Goto A, Nunoi Y, Izumi-Nakaseko H, Chiba K, Wada T, Takei Y, Matsumoto A, and Sugiyama A (2021b) Analysis of electropharmacological and proarrhythmic effects of donepezil using the halothane-anesthetized intact dogs and the conscious chronic atrioventricular block ones. Naunyn Schmiedeberg Arch Pharmacol 934: 581-589.

Hondeghem LM, Carlsson L, and Duker G (2001) Instability and triangulation of the action potential predict serious proarrhythmia, but action potential duration prolongation is antiarrhythmic. Circulation 103: 2004-2013.

Hondeghem LM, and Hoffmann P (2003) Blinded test in isolated female rabbit heart

reliably identifies action potential duration prolongation and proarrhythmic drugs: importance of triangulation, reverse use dependence, and instability. J Cardiovasc Pharmacol 41: 14-24.

Hornyik T, Castiglione A, Franke G, Perez-Feliz S, Major P, Hiripi L, Koren G, Bősze Z, Varró A, Zehender M, Brunner M, Bode C, Baczkó, and Odening K.E (2020) Transgenic LQT2, LQT5, and LQT2-5 rabbit models with decreased repolarisation reserve for prediction of drug-induced ventricular arrhythmias. Br J Pharmacol 177: 3744-3759.

Iida T, Morimoto S, Amari Y, Ando T, and Ichihara A (2017) Effects of L- and N-type Ca channel blocker cilnidipine on changes in heart rate and QT interval during dialysis. Kidney Blood Press Res 42: 933-941.

Inaba H, Hayami N, Ajiki K, Sugishita Y, Kunishima T, Yamagishi N, Yamagishi S, and Murakawa Y (2008) Human atrial natriuretic peptide suppresses torsades de pointes in rabbits. Circ J 72: 820-824.

Ishizaka T, Takahara A, Iwasaki H, Mitsumori Y, Kise H, Nakamura Y, and Sugiyama A (2008) Comparison of electropharmacological effects of bepridil and sotalol in the halothane-anesthetized dogs. Circ J 72: 1003-1011.

Iwasaki H, Takahara A, Nakamura Y, Satoh Y, Nagai T, Shinkai N, and Sugiyama A

(2009) Simultaneous assessment of pharmacokinetics of pilsicainide transdermal patch and its electropharmacological effects on atria of chronic atrioventricular block dogs. J Pharmacol Sci 110: 410-414.

Izumi-Nakaseko H, Nakamura Y, Cao X, Ohara H, Yamazaki Y, Ueda N, Ando K, and Sugiyama A (2014) Effects of selective I_{Kr} channel blockade by E-4031 on ventricular electro-mechanical relationship in the halothane-anesthetized dogs. Eur J Pharmacol 740: 263-270.

Izumi-Nakaseko H, Nakamura Y, Cao X, Wada T, Ando K, and Sugiyama A (2016) Possibility as an anti-cancer drug of astemizole: evaluation of arrhythmogenicity by the chronic atrioventricular block canine model. J Pharmacol Sci 131: 150-153.

Izumi-Nakaseko H, Kanda Y, Nakamura Y, Hagiwara M, Wada T, Ando K, Naito AT, Sekino Y, and Sugiyama A (2017a) Development of correction formula for field potential duration of human induced pluripotent stem cell-derived cardiomyocytes sheets. J Pharmacol Sci 135: 44-50.

Izumi-Nakaseko H, Nakamura Y, Cao X, Wada T, Ando K, and Sugiyama A (2017b) Assessment of safety margin of an antipsychotic drug haloperidol for torsade de pointes using the chronic atrioventricular block dogs. Cardiovasc Toxicol

17: 319-325.

Izumi-Nakaseko H, Nakamura Y, Wada T, Ando K, Kanda Y, Sekino Y, and Sugiyama A (2017c) Characterization of human iPS cell-derived cardiomyocyte sheets as a model to detect drug-induced conduction disturbance. J Toxicol Sci 42: 183-192.

Izumi-Nakaseko H, Hagiwara-Nagasawa M, Naito AT, Goto A, Chiba K, Sekino Y, Kanda Y, and Sugiyama A (2018) Application of human induced pluripotent stem cell-derived cardiomyocytes sheets with microelectrode array system to estimate antiarrhythmic properties of multi-ion channel blockers. J Pharmacol Sci 137: 372-378.

Izumi-Nakaseko H, Chiba K, Hagiwara-Nagasawa M, Satsuka A, Goto A, Nunoi Y, Kambayashi R, Matsumoto A, Takei Y, Kanda Y, Naito AT, and Sugiyama A (2020a) Optimizing the direction and order of the motion unveiled the ability of conventional monolayers of human induced pluripotent stem cell-derived cardiomyocytes to show frequency-dependent enhancement of contraction and relaxation motion. Front Cell Dev Biol 8: 542562.

Izumi-Nakaseko H, Fujiyoshi M, Hagiwara-Nagasawa M, Goto A, Chiba K, Kambayashi R, Naito AT, Ando K, Kanda Y, Ishii I, and Sugiyama A (2020b)

Dasatinib can impair left ventricular mechanical function but may lack proarrhythmic effect: a proposal of non-clinical guidance for predicting clinical cardiovascular adverse events of tyrosine kinase inhibitors. Cardiovasc Toxicol 20: 58-70.

Izumi-Nakaseko H, Chiba K, Goto A, Kambayashi R, Matsumoto A, Takei Y, Kawai S, and Sugiyama A (2023a) Electropharmacological characterization of licorice using the human induced pluripotent stem cell-derived cardiomyocytes sheets and the chronic atrioventricular block dogs. Cardiovasc Toxicol 23: 207-217.

Izumi-Nakaseko H, Sakamoto K, Goto A, Kambayashi R, Matsumoto A, Takei T, Takahara A, and Sugiyama A (2023b) Characterization of pathological remodeling in the chronic atrioventricular block cynomolgus monkey heart. Front Pharmacol 14: 1055031.

Jia S, Lian J, Guo D, Xue X, Patel C, Yang L, Yuan Z, Ma A, and Yan GX (2011) Modulation of the late sodium current by ATX-II and ranolazine affects the reverse use-dependence and proarrhythmic liability of I_{Kr} blockade. Br J Pharmacol 164: 308-316.

Johannesen L, Vicente J, Gray RA, Galeotti L, Loring Z, Garnett CE, Florian J, Ugander M, Stockbridge N, and Strauss DG (2014a) Improving the assessment

of heart toxicity for all new drugs through translational regulatory science. Clin Pharmacol Ther 95: 501-508.

Johannesen L, Vicente J, Mason JW, Scanabria C, Waite-Labott K, Hong M, Guo P, Lin J, Sørensen JS, Galeotti L, Florian J, Ugander M, Stockbridge N, and Strauss DG (2014b) Differentiating drug-induced multichannel block on the electrocardiogram: randomized study of dofetilide, quinidine, ranolazine, and verapamil. Clin Pharmaco Ther 96: 549-558.

Kambayashi R, Hagiwara-Nagasawa M, Goto A, Chiba K, Izumi-Nakaseko H, Naito AT, Matsumoto A, and Sugiyama A (2020a) Experimental analysis of the onset mechanism of TdP reported in an LQT3 patient during pharmacological treatment with serotonin-dopamine antagonists against insomnia and nocturnal delirium. Heart Vessels 35: 593-602.

Kambayashi R, Hagiwara-Nagasawa M, Ichikawa T, Goto A, Chiba K, Nunoi Y, Izumi-Nakaseko H, Matsumoto A, Takahara A, and Sugiyama A (2020b) Analysis of electropharmacological effects of AVE0118 on the atria of chronic atrioventricular block dogs: characterization of anti-atrial fibrillatory action by atrial repolarization-delaying agent. Heart Vessels 35: 1316-1322.

Kambayashi R, Izumi-Nakaseko H, Goto A, Tsurudome K, Ohshiro H, Izumi T,

Hagiwara-Nagasawa M, Chiba K, Nishiyama R, Oyama S, Nunoi Y, Takei Y, Matsumoto A, and Sugiyama A (2021a) Translational studies on anti-atrial fibrillatory action of oseltamivir by its in vivo and in vitro electropharmacological analyses. Front Pharmacol 396: 1103-1112.

Kambayashi R, Goto A, Nunoi Y, Hagiwara-Nagasawa M, Izumi-Nakaseko H, Venkatesan G, Takei Y, Matsumoto A, Chan ECY, and Sugiyama A (2021b) An exploratory analysis of effects of poyendarone, a deuterated analogue of dronedarone, on the canine model of paroxysmal atrial fibrillation. Naunyn Schmiedebergs Arch Pharmacol 394: 1103-1112.

Kambayashi R, Goto A, Hagiwara-Nagasawa M, Izumi-Nakaseko H, Shinozaki M, Kawai S, Matsumoto A, Takei Y, and Sugiyama A (2022a) Analysis of clinically-reported, memantine-induced cardiovascular adverse responses using the halothane-anesthetized dogs: reverse translational study. J Pharmacol Sci 148: 343-350.

Kambayashi R, Goto A, Izumi-Nakaseko H, Takei Y, Matsumoto A, Kawai S, and Sugiyama A (2022b) Roles of $I_{K,ACh}$ for perpetuating atrial fibrillation: effects of atrial-selective K^+ channel inhibitor AVE0118 and class I drugs on the persistent atrial fibrillation canine model. J Pharmacol Sci 149: 175 -178.

Kambayashi R, Goto A, Onozato M, Izumi-Nakaseko H, Takei Y, Matsumoto A, Kawai S, Fukushima T, and Sugiyama A (2022c) Simultaneous analyses of hemodynamic and electrophysiological effects of oseltamivir along with its pharmacokinetic profile using the canine paroxysmal atrial fibrillation model. J Pharmacol Sci 148: 179-186.

Kambayashi R, Goto A, Izumi-Nakaseko H, Takei Y, and Sugiyama A (2024) Characterization of cardiovascular profile of anti-influenza drug peramivir: a reverse-translational study using the isoflurane-anesthetized dog. J Pharmacol Sci 154: 218-224.

Kaneko N, Itoh K, Sugiyama A, and Izumi Y (2011) Microminipig, a non-rodent experimental animal optimized for life scienceresearch. Preface. J Pharmacol Sci 115: 112-114.

Kannankeril P, Roden DM, and Darbar D (2010) Drug-induced long QT syndrome. Pharmacol Rev 62: 760-781.

Karkhanis AV, Venkatesan G, Kambayashi R, Leow JWH, Han MQ, Izumi-Nakaseko H, Goto A, Pang JKS, Soh BS, Kojodjojo P, Sugiyama A, and Chan ECY (2022) Site-directed deuteration of dronedarone preserves cytochrome P4502J2 activity and mitigates its cardiac adverse effects in canine arrhythmic hearts.

Acta pharmaceutica Sinica B 12: 3905-3923.

Kawakami S, Nagasawa Y, Hagiwara-Nagasawa M, Omura K, Aimoto M, and Takahara A (2020) Torsadogenic potential of a novel remyelinating drug clemastine for multiple sclerosis assessed in the rabbit proarrhythmia model. J Pharmacol Sci 144: 123-128.

Kawakami S, Kambayashi R, Takada K, Aimoto M, Nagasawa Y, and Takahara A (2022) Role of cardiac α_1-adrenoreceptors for the torsadogenic action of I_{Kr} blocker nifekalant in the anesthetized atrioventricular block rabbit. J Pharmacol Sci 150: 67-73.

Kawakami S, Takada K, Aimoto M, Nagasawa Y, Kusakabe T, Kato K, and Takahara A (2023) The antiarrhythmic action of the Na^+/Ca^{2+} exchanger inhibitor SEA0400 on drug-induced long QT syndrome depends on the severity of proarrhythmic conditions in anesthetized atrioventricular block rabbits. Biol Pharm Bull 46: 1120-1127.

Kitahara K, Nakamura Y, Tsuneoka Y, Adachi-Akahane S, Tanaka H, Yamazaki H, Takahara A, Yamazaki J, Ikeda T, and Sugiyama A (2013) Cardiohemodynamic and electrophysiological effects of anti-influenza drug oseltamivir in vivo and in vitro. Cardiovasc Toxicol 13: 234-243.

Komatsu R, Mizuno H, Ishizaka T, Ito A, Jikuzono T, Kakoi T, Bando M, Koga T, Handa J, Takahashi Y, Kanno A, Ozaki H, Chiba K, and Japan activity for Improvement of Cardiovascular Evaluation by Telemetry system (J-ICET) (2019) Exposure-response analysis of drug-induced QT interval prolongation in telemetered monkeys for translational prediction to human. J Pharmacol Toxicol Methods 99: 106606.

Kondo Y, Hagiwara-Nagasawa M, Kambayashi R, Goto A, Chiba K, Nunoi Y, Izumi-Nakaseko H, Matsumoto A, and Sugiyama A (2020) Electropharmacological characterization of aciclovir in the halothane-anesthetized dogs: a proposal of evaluation method for cardiovascular safety pharmacology of anti-virus drugs. Cardiovascr Toxicol 20: 419-426.

Laursen M, Grunnet M, Olesen SP, Jespersen T, and Mow T (2011) Keeping the rhythm – Pro-arrhythmic investigations in isolated Göttingen minipig hearts. J Pharmacol Toxicol Meth 64: 134-144.

Lawrence CL, Bridgland-Taylor MH, Pollard CE, Hammond TG, and Valentin JP (2006) A rabbit Langendorff heart proarrhythmia model: predictive value for clinical identification of torsades de pointes. Br J Pharmacol 149: 845-860.

Li Z, Ridder BJ, Han X, Wu WW, Sheng J, Tran PN, Wu M, Randolph A, Johnstone RH, Mirams GR, Kuryshev Y, Kramer J, Wu C, Crumb Jr WJ, and Strauss DG (2019) Assessment of an in silico mechanistic model for proarrhythmia risk prediction under the CiPA Initiative. Clin Pharmacol Ther 105: 466-475.

Liu T, Brown BS, Wu Y, Antzelevitch C, Kowey PR, and Yan GX (2006) Blinded validation of the isolated arterially perfused rabbit ventricular wedge in preclinical assessment of drug-induced proarrhythmias. Heart Rhythm 3: 948-956.

Liu T, Liu J, Lu HR, Li H, Gallacher DJ, Chaudhary K, Wang Y, and Yan GX (2021) Utility of normalized TdP score system in drug proarrhythmic potential assessment: a blinded in vitro study of CiPA drugs. Clin Pharmacol Ther 109: 1606-1617.

Llopis-Lorente J, Baroudi S, Koloskoff K, Mora MT, Basset M, Romero L, Benito S, Dayan F, Saiz J, and Trenor B (2023) Combining pharmacokinetic and electrophysiological models for early prediction of drug-induced arrhythmogenicity. Comput Methods Programs Biomed 242: 107860.

Loen V, Vos MA, and van der Heyden MAG (2022) The canine chronic atrioventricular block model in cardiovascular preclinical drug research. Br J Pharmacol 179:

859-881.

Lu HR, Remeysen P, and De Clerck F (2000) Nonselective I_{Kr}-blockers do not induce torsades de pointes in the anesthetized rabbit during α_1-adrenoceptor stimulation. J Cardiovasc Pharmacol 36: 728-736.

Lu HR, Vlaminckx E, Van de Water A, Rohrbacher J, Hermans A, and Gallacher DJ (2007) Corrigendum to "In-vitro experimental models for the risk assessment of antibiotic-induced QT prolongation". Eur J Pharmacol 577: 222-232.

Lu Z, Kamiya K, Opthof T, Yasui K, and Kodama I (2001) Density and kinetics of I_{Kr} and I_{Ks} in guinea pig and rabbit ventricular myocytes explain different efficacy of I_{Ks} blockade at high heart rate in guinea pig and rabbit: implications for arrhythmogenesis in humans. Circulation 104: 951-956.

Major P, Baczkó I, Hiripi L, Odening KE, Juhász V, Kohajda Z, Horváth A, Seprényi G, Kovács M, Virág L, Jost N, Prorok J, Ördög B, Doleschall Z, Nattel S, Varró A, and Bősze Z (2016) A novel transgenic rabbit model with reduced repolarization reserve: long QT syndrome caused by a dominant-negative mutation of the KCNE1 gene. Br J Pharmacol 173: 2046-2061.

Marx SO, Kurokawa J, Reiken S, Motoike H, D'Armiento J, Marks AR, and Kass RS (2002) Requirement of a macromolecular signaling complex for beta

adrenergic receptor modulation of the KCNQ1-KCNE1 potassium channel. Science 295: 496-499.

Matsukura S, Nakamura Y, Cao X, Wada T, Izumi-Nakaseko H, Ando K, and Sugiyama A. (2017) Anti-atrial fibrillatory versus proarrhythmic potentials of amiodarone: a new protocol for safety evaluation in vivo. Cardiovasc Toxicol 17: 157-162.

Matsuo J, Nakamura Y, Izumi-Nakaseko H, Ando K, Sekino Y, and Sugiyama A (2015) Possible effects of inhibition of I_{Kr} and I_{Ks} on field-potential waveforms in the human iPS cell-derived cardiomyocytes sheet. J Pharmacol Sci 128: 92-95.

Milberg P, Eckardt L, Bruns HJ, Biertz J, Ramtin S, Reinsch N, Fleischer D, Kirchhof P, Fabritz L, Breithardt G, and Haverkamp W (2002) Divergent proarrhythmic potential of macrolide antibiotics despite similar QT prolongation: fast phase 3 repolarization prevents early afterdepolarizations and torsade de pointes. J Pharmacol Exp Ther 303: 218-225.

Milberg P, Hilker E, Ramtin S, Cakir Y, Stypmann J, Engelen MA, Mönnig G, Osada N, Breithardt G, Haverkamp W, and Eckardt L (2007) Proarrhythmia as a class effect of quinolones: increased dispersion of repolarization and triangulation of action potential predict torsades de pointes. J Cardiovasc Electrophysiol 18:

647-654.

Motokawa Y, Nakamura Y, Hagiwara-Nagasawa M, Goto A, Chiba K, Lubna NJ, Izumi-Nakaseko H, Ando K, Naito AT, Yamazaki H, and Sugiyama A (2018) In vivo analysis of the anti-atrial fibrillatory, proarrhythmic and cardiodepressive profiles of dronedarone as a guide for safety pharmacological evaluation of antiarrhythmic drugs. Cardiovasc Toxicol 18: 242-251.

Nakamura Y, Matsuo J, Miyamoto N, Ojima A, Ando K, Kanda Y, Sawada K, Sugiyama A, and Sekino Y (2014) Assessment of testing methods of the drug-induced repolarization delay and arrhythmias in an iPS cell-derived cardiomyocyte sheet: multi-site validation study. J Pharmacol Sci 124: 494-501.

Nakamura Y, Sasaki R, Cao X, Wada T, Hamaguchi S, Izumi-Nakaseko H, Ando K, Tanaka H, Takahara A, and Sugiyama A (2016) Intravenous anti-influenza drug oseltamivir will not induce torsade de pointes: Evidence from proarrhythmia model and action-potential assay. J Pharm Sci 131: 72-75.

Nakaya H, Tohse N, Takeda Y, and Kanno M (1993) Effects of MS-551, a new class III antiarrhythmic drug, on action potential and membrane currents in rabbit ventricular myocytes. Br J Pharmacol 109: 157-163.

Nunoi Y, Chiba K, Hagiwara-Nagasawa M, Goto A, Kambayashi R, Izumi-Nakaseko H,

Takei Y, Matsumoto A, Watanabe Y, and Sugiyama A (2020) Risperidone alone did not induce torsade de pointes: experimental evidence from the chronic atrioventricular block model dogs. J Pharmacol Sci 43: 330-332.

Nunoi Y, Kambayashi R, Goto A, Hagiwara-Nagasawa M, Chiba K, Izumi-Nakaseko H, Kawai S, Takei Y, Matsumoto A, Watanabe Y, and Sugiyama A (2021) In vivo characterization of anti-atrial fibrillatory potential and pharmacological safety profile of $I_{Na,L}$ plus I_{Kr} inhibitor ranolazine using the halothane-anesthetized dogs. Heart Vessels 36: 1088-1097.

Obejero-Paz CA, Bruening-Wright A, Kramer J, Hawryluk P, Tatalovic M, Dittrich HC, and Brown AM (2015) Quantitative profiling of the effects of vanoxerine on human cardiac ion channels and its application to cardiac risk. Sci Rep 5: 17623.

Ohara H, Nakamura Y, Watanabe Y, Cao X, Yamazaki Y, Izumi-Nakaseko H, Ando K, Yamazaki H, Yamazaki J, Ikeda T, and Sugiyama A (2015) Azithromycin can prolong QT interval and suppress ventricular contraction, but will not induce torsade de pointes. Cardiovasc Toxicol 15: 232-240.

Oros A, Volders PG, Beekman JD, van der Nagel T, and Vos MA (2006) Atrial-specific drug AVE0118 is free of torsades de pointes in anesthetized dogs with chronic

complete atrioventricular block. Heart Rhythm 3: 1339-1345.

Oros A, Houtman MJ, Neco P, Gomez AM, Rajamani S, Oosterhoff P, Attevelt NJ, Beekman JD, van der Heyden MA, Ver Donck L, Belardinelli L, Richard S, Antoons G, and Vos MA (2010) Robust anti-arrhythmic efficacy of verapamil and flunarizine against dofetilide-induced TdP arrhythmias is based upon a shared and a different mode of action. Br J Pharmacol 161: 162-175.

Piccini JP, Pritchett EL, Davison BA, Cotter G, Wiener LE, Koch G, Feld G, Waldo A, van Gelder IC, Camm AJ, Kowey PR, Iwashita J, and Dittrich HC (2016) Randomized, double-blind, placebo-controlled study to evaluate the safety and efficacy of a single oral dose of vanoxerine for the conversion of subjects with recent onset atrial fibrillation or flutter to normal sinus rhythm: RESTORE SR. Heart Rhythm 13: 1777-1783.

Rossman EI, Wisialowski TA, Vargas HM, Valentin JP, Rolf MG, Roche BM, Riley S, Pugsley MK, Nichols J, Li D, Leishman DJ, Kleiman RB, Greiter-Wilke A, Gintant GA, Engwall MJ, Delaunois A, and Authier S (2023) Best practice considerations for nonclinical in vivo cardiovascular telemetry studies in non-rodent species: Delivering high quality QTc data to support ICH E14/S7B Q&As. J Pharmacol Toxicol Methods 123:107270.

Sager PT, Gintant G, Turner JR, Pettit S, and Stockbridge N (2014) Rechanneling the cardiac proarrhythmia safety paradigm: a meeting report from the Cardiac Safety Research Consortium. Am Heart J 167: 292-300.

Satoh Y, Sugiyama A, Takahara A, and Hashimoto K (2004) Electropharmacological and proarrhythmic effects of a class III antiarrhythmic drug nifekalant hydrochloride assessed using the *in vivo* canine models. J Cardiovasc Pharmacol 43: 715-723.

Satoh Y, Sugiyama A, Takahara A, Ando K, Wang K, Honsho S, and Hashimoto K (2005) An antipsychotic and antiemetic drug prochlorperazine delays the ventricular repolarization of the in situ canine heart. J Pharmacol Sci 97: 101-106.

Shimizu W and Antzelevitch C (1997) Sodium channel block with mexiletine is effective in reducing dispersion of repolarization and preventing torsade de pointes in LQT2 as well as LQT3 models of the long QT syndrome. Circulation 96: 2038-2047.

Shimizu W, McMahon B, and Antzelevitch C (1999) Sodium pentobarbital reduces transmural dispersion of repolarization and prevents torsades de pointes in models of acquired and congenital long QT syndrome. J Cardiovasc

Electrophysiol 10: 154-164.

Sicouri S, Moro S, Litovsky S, Elizari MV, and Antzelevitch C (1997) Chronic amiodarone reduces transmural dispersion of repolarization in the canine heart. J Cardiovasc Electrophysiol 8: 1269-1279.

Sossalla S, Wallisch N, Toischer K, Sohns C, Vollmann D, Seegers J, Lüthje L, Maier LS, and Zabel M (2014) Effects of ranolazine on torsades de pointes tachycardias in a healthy isolated rabbit heart model. Cardiovasc Ther 32: 170-177.

Steidl-Nichols JV, Hanton G, Leaney J, Liu RC, Leishman D, McHarg A, and Wallis R (2008) Impact of study design on proarrhythmia prediction in the SCREENIT rabbit isolated heart model. J Pharmacol Toxicol Methods 57: 9-22.

Strauss DG, Wu WW, Li Z, Koerner J, and Garnett C (2021) Translational Models and Tools to Reduce Clinical Trials and Improve Regulatory Decision Making for QTc and Proarrhythmia Risk (ICH E14/S7B Updates). Clin Pharmacol Ther 109: 319-333.

Sugiyama A (2008) Sensitive and reliable proarrhythmia in vivo animal models for predicting drug-induced torsades de pointes in patients with remodelled hearts. Br J Pharmacol 154: 1528-1537.

Sugiyama A, Motomura S, and Hashimoto K (1994) Utilization of isolated, blood-perfused canine papillary muscle preparation as a model to assess efficacy and adversity of class I antiarrhythmic drugs. Jpn J Pharmacol 66: 303-316.

Sugiyama A, and Hashimoto K (2002) Effects of a typical I_{Kr} channel blocker sematilide on the relationship between ventricular repolarization, refractoriness and onset of torsades de pointes. Jpn J Pharmacol 88: 414-421.

Sugiyama A, Ishida Y, Satoh Y, Aoki S, Hori M, Akie Y, Kobayashi Y, and Hashimoto K (2002a) Electrophysiological, anatomical and histological remodeling of the heart to AV block enhances susceptibility to arrhythmogenic effects of QT prolonging drugs. Jpn J Pharmacol 88: 341-350.

Sugiyama A, Satoh Y, Ishida Y, Yoneyama M, Yoshida H, and Hashimoto K (2002b) Pharmacological and electrophysiological characterization of junctional rhythm during radiofrequency catheter ablation of the atrioventricular node: possible involvement of neurotransmitters from autonomic nervous system. Circ J 66: 696-701.

Sugiyama A, Satoh Y, Shiina H, Takeda S, and Hashimoto K (2002c) Torsadegenic action of the antipsychotic drug sulpiride assessed using in vivo canine models.

J Cardiovasc Pharmacol 40: 235-245.

Sugiyama A, Satoh Y, Takahara A, Nakamura Y, Shimizu-Sasamata M, Sato S, Miyata K, and Hashimoto K (2003) Famotidine does not induce long QT syndrome: experimental evidence from in vitro and in vivo test systems. Eur J Pharmacol 466: 137-146.

Sugiyama A, Nakamura Y, Akie Y, Saito H, Izumi Y, Yamazaki H, Kaneko N, and Itoh K (2011) Microminipig, a non-rodent experimental animal optimized for life science research. In vivo proarrhythmia models of drug-induced long QT syndrome: development of chronic atrioventricular block model of microminipig. J Pharmacol Sci 115: 122-126.

Sugiyama A, Hagiwara-Nagasawa M, Kambayashi R, Goto A, Chiba K, Naito AT, Kanda Y, Matsumoto A, and Izumi-Nakaseko H (2019) Analysis of electro-mechanical relationship in human iPS cell-derived cardiomyocytes sheets under proarrhythmic condition assessed by simultaneous field potential and motion vector recordings. J Pharmacol Sciences 140: 317-320.

Suzuki N, Kambayashi R, Goto A, Izumi-Nakaseko H, Takei Y, Naito AT, and Sugiyama A (2023) Cardiovascular safety pharmacology of ivermectin assessed using the isoflurane-anesthetized beagle dogs: ICH S7B follow-up study. J Toxicol Sci

48: 645-654.

Tabo M, Komatsu R, Isobe T, Honda M, Yamada Y, and Kimura K (2010) Accurate detection of drug-induced delayed ventricular repolarization with a suitable correction formula in Langendorff guinea pig heart. J Toxicol Sci 35: 687-698.

Takahara A, Sugiyama A, Ishida Y, Wang K, Nakamura Y, and Hashimoto K (2006) Long-term bradycardia caused by atrioventricular block can remodel the canine heart to detect the histamine H_1 blocker terfenadine-induced torsades de pointes arrhythmias. Br J Pharmacol 147: 634-641.

Takahara A, Nakamura H, Nouchi H, Tamura T, Tanaka T, Shimada H, Tamura M, Tsuruoka N, Takeda K, Tanaka H, Shigenobu K, Hashimoto K, and Sugiyama A (2007) Analysis of arrhythmogenic profile in a canine model of chronic atrioventricular block by comparing in vitro effects of the class III antiarrhythmic drug nifekalant on the ventricular action potential indices between normal heart and atrioventricular block heart. J Pharmacol Sci 103: 181-188.

Takahara A, Nakamura Y, and Sugiyama A (2008) Beat-to-beat variability of repolarization differentiates the extent of torsadogenic potential of multi ion channel-blockers bepridil and amiodarone. Eur J Pharmacol 596: 127-131.

Takahara A, Nakamura Y, Wagatsuma H, Aritomi S, Nakayama A, Satoh Y, Akie Y, and Sugiyama A (2009) Long-term blockade of L/N-type Ca^{2+} channels by cilnidipine ameliorates repolarization abnormality of the canine hypertrophied heart. Br J Pharmacol 158: 1366-1374.

Thomsen MB, Verduyn SC, Stengl M, Beekman JD, de Pater G, van Opstal J, Volders PG, and Vos MA (2004) Increased short-term variability of repolarization predicts d-sotalol-induced torsades de pointes in dogs. Circulation 110: 2453-2459.

Thomsen MB, Beekman JD, Attevelt NJ, Takahara A, Sugiyama A, Chiba K, and Vos MA (2006) No proarrhythmic properties of the antibiotics Moxifloxacin or Azithromycin in anaesthetized dogs with chronic-AV block. Br J Pharmacol 149: 1039-1048.

Tsuji Y, Opthof T, Yasui K, Inden Y, TakemuratH, Niwa N, Lu Z, Lee JK, Honjo H, Kamiya K, and Kodama I (2002) Ionic mechanisms of acquired QT prolongation and torsades de pointes in rabbits with chronic complete atrioventricular block. Circulation 106: 2012-2018.

Tsuji Y, Hojo M, Voigt N, El-Armouche A, Inden Y, Murohara T, Dobrev D, Nattel S, Kodama I, and Kamiya K (2011) Ca^{2+}-related signaling and protein

phosphorylation abnormalities play central roles in a new experimental model of electrical storm. Circulation 123: 2192-2203.

Van de Water A, Verheyen J, Xhonneux R, and Reneman RS (1989) An improved method to correct the QT interval of the electrocardiogram for changes in heart rate. J Pharmacol Methods 22: 207-217.

van Opstal JM, Leunissen JD, Wellens HJ, and Vos MA (2001a) Azimilide and dofetilide produce similar electrophysiological and proarrhythmic effects in a canine model of Torsade de Pointes arrhythmias. Eur J Pharmacol 412: 67-76.

van Opstal JM, Schoenmakers M, Verduyn SC, de Groot SH, Leunissen JD, van Der Hulst FF, Molenschot MM, Wellens HJ, and Vos MA (2001b) Chronic amiodarone evokes no torsade de pointes arrhythmias despite QT lengthening in an animal model of acquired long-QT syndrome. Circulation 104: 2722-2727.

Vargas HM, Rossman EI, Wisialowski TA, Nichols J, Pugsley MK, Roche B, Gintant GA, Greiter-Wilke A, Kleiman RB, Valentin JP, and Leishman DJ (2023) Improving the in Vivo QTc assay: The value of implementing best practices to support an integrated nonclinical-clinical QTc risk assessment and TQT substitute. J Pharmacol Toxicol Methods 121:107265.

Varró A, and Baczkó I (2011) Cardiac ventricular repolarization reserve: a principle for understanding drug-related proarrhythmic risk. Br J Pharmacol 164: 14-36.

Vos MA (2008) Literature-based evaluation of four 'hard endpoint' models for assessing drug-induced torsades de pointes liability. Br J Pharmacol 154: 1523-1527.

Wada T, Ando K, Naito AT, Nakamura Y, Goto A, Chiba K, Lubnaa NJ, Cao X, Hagiwara-Nagasawa M, Izumi-Nakaseko H, Nakazato Y, and Sugiyama A (2018) Sunitinib does not acutely alter left ventricular systolic function but induces diastolic dysfunction. Cancer Chemother Pharmacol 82: 65-75.

Watanabe Y, Nakamura Y, Cao X, Ohara H, Yamazaki Y, Murayama N, Sugiyama Y, Izumi-Nakaseko H, Ando K, Yamazaki H, and Sugiyama A (2015) Intravenous administration of apomorphine does not induce long QT syndrome: experimental evidence from in vivo canine models. Basic Clin Pharmacol Toxicol 116: 468-475.

Watson KJ, Gorczyca WP, Umland J, Zhang Y, Chen X, Sun SZ, Fermini B, Holbrook M, and Van Der Graaf PH (2011) Pharmacokinetic-pharmacodynamic modeling of the effect of moxifloxacin on QTc prolongation in telemetered cynomolgus monkeys. J Pharmacol Toxicol Methods 63: 304-313.

Woosley RL, Heise CW, Gallo T, Woosley D and Romero KA, www.CredibleMeds.org,

QTdrugs List, Accessed February 12, 2024, AZCERT, Inc. 1457 E. Desert Garden Dr., Tucson, AZ 85718.

Yamamoto W, Asakura K, Ando H, Taniguchi T, Ojima A, Uda T, Osada T, Hayashi S, Kasai C, Miyamoto N, Tashibu H, Yoshinaga T, Yamazaki D, Sugiyama A, Kanda Y, Sawada K, and Sekino Y (2016) Electrophysiological characteristics of human iPS-derived cardiomyocytes for the assessment of drug-induced proarrhythmic potential. PLoS One 11: e0167348.

Yamazaki D, Kitaguchi T, Ishimura M, Taniguchi T, Yamanishi A, Saji D, Takahashi E, Oguchi M, Moriyama Y, Maeda S, Miyamoto K, Morimura K, Ohnaka H, Tashibu H, Sekino Y, Miyamoto N, and Kanda Y (2018) Proarrhythmia risk prediction using human induced pluripotent stem cell-derived cardiomyocytes. J Pharmacol Sci 136: 249-256.

Yokoyama H, Nakamura Y, Saito H, Nagayama Y, Hoshiai K, Wada T, Izumi-Nakaseko H, Ando K, Akie Y, and Sugiyama A (2017) Pharmacological characterization of microminipig as a model to assess the drug-induced cardiovascular responses for non-clinical toxicity and/or safety pharmacology studies. J Toxicol Sci 42: 93-101.

Yoshida H, Sugiyama A, Satoh Y, Ishida Y, Yoneyama M, Kugiyama K, and Hashimoto

K (2002) Comparison of in vivo electrophysiological and proarrhythmic effects of amiodarone with those of a selective class III drug sematilide using the canine chronic AV block model. Circ J 66: 758-762.

Zabel M, Hohnloser SH, Behrens S, Woosley RL, and Franz MR (1997) Differential effects of D-sotalol, quinidine, and amiodarone on dispersion of ventricular repolarization in the isolated rabbit heart. J Cardiovasc Electrophysiol 8: 1239-1245.

Footnotes.

This study was supported in part by JSPS KAKENHI Grant Numbers 20K16136 to R.K., 23K08430 to A.S. and 23K15143 to A.G.

Conflict of interest:

The authors declare no potential conflicts of interest.

Corresponding author.

Atsushi Sugiyama, MD, PhD

Department of Pharmacology, Faculty of Medicine, Toho University

5-21-16 Omori-nishi, Ota-ku, Tokyo 143-8540, Japan

E-mail: atsushi.sugiyama@med.toho-u.ac.jp

JPET Fast Forward. Published on August 21, 2024 as DOI: 10.1124/jpet.124.002184
This article has not been copyedited and formatted. The final version may differ from this version.

Figure legends

Fig. 1

A causal relationship between the I_{Kr} channel blockade in vitro and the onset of adverse events including QT-interval prolongation and torsade de pointes (TdP) in patients. Since there are wide variations in the sensitivity toward I_{Kr} channel blockers among the patients, I_{Kr} channel blockers do not always prolong QT interval or induce lethal arrhythmia TdP. Indeed, such serious adverse events may not happen to most of the patients (blue arrow) but can be induced in only a small number of patients (red arrow).

Fig. 2

Onset mechanism of drug-induced torsade de pointes in patients. I_{Kr} channel blocker is distributed to the in situ heart that the autonomic nervous system regulates. In the heart with reduced repolarization reserve, I_{Kr} channel blocker will induce excessive QT-interval prolongation, providing both trigger and substrate toward the onset of torsade de pointes. The trigger includes temporal dispersion of repolarization, leading to the onset of R on T-type premature ventricular contraction (PVC). Meanwhile, the substrate indicates spatial dispersion of repolarization and local electrical vulnerability

in the ventricles. Using this concept, several proarrhythmic surrogate markers have been devised. For example, J-T_{peak} can predict the degree of Ca^{2+} overload in myocardial cells that causes the temporal dispersion, which can be quantified by short-term variability (STV) of repolarization. Meanwhile, T_{peak}-T_{end} reflects the transmural dispersion of ventricular repolarization for initiating spiral re-entry, whereas terminal repolarization period (TRP) predicts the local ventricular electrical vulnerability for perpetuating reentrant circuits.

Fig. 3

Schematic representation of action potentials (top panels) and corresponding electrocardiogram (bottom panels) at control (left panels), I_{Kr} inhibition alone (middle panels) and multi-channel inhibition with increased sympathetic tone (right panels). I_{Kr} inhibition prolongs both the early (J-T_{peak}) and late (T_{peak}-T_{end}) repolarization periods of the ventricle (middle bottom panel). J-T_{peak} can estimate the net balance between inward I_{CaL} plus I_{NaL} and outward I_{Ks} plus I_{Kr}, governing "trigger" of the premature ventricular contractions, whereas T_{peak}-T_{end} may reflect the extent of I_{Kr} modification along with the transmural dispersion of ventricular repolarization, providing "substrate" for the initiation of torsade de pointes. Inhibition of I_{CaL} and I_{NaL} with an enhancement

JPET Fast Forward. Published on August 21, 2024 as DOI: 10.1124/jpet.124.002184
This article has not been copyedited and formatted. The final version may differ from this version.

of I_{Ks} by hypotension-induced increase of sympathetic tone (right top panel, blue arrows) may counterbalance I_{Kr} inhibition (right top panel, red arrow), resulting in negligible change in QT interval, the so-called, balanced multi-channel block (right bottom panel).

Fig. 4

Extent of the repolarization reserve in humans and animal models. While the number of red boxes indicates the amount of minimum functional unit of K^+ channels required for maintaining a normal ventricular repolarization period, the number of blue boxes represents the amount of repolarization reserve. For example, conscious animals (monkeys and dogs) have more repolarization reserves than healthy human subjects. The amount of repolarization reserve in healthy human subjects is similar to that in dogs anesthetized with halothane or isoflurane. The amount of repolarization reserve decreases in patients at high risk, which can be reproduced by chronic atrioventricular (AV) block dogs and monkeys.

Fig. 5

Ca^{2+} dynamics (top panels), action potential (middle panels) and electrocardiogram

(bottom panels) in the absence (left panels) and presence (right panels) of tyrosine kinase inhibitor (TKI). TKI can impair the mitochondrial function, reducing ATP production, which may suppress sarcoplasmic/endoplasmic reticulum Ca^{2+} ATPase (SERCA) activity as well as sarcolemmal Ca^{2+} pump function. The SERCA and sarcolemmal Ca^{2+} pump inhibition could increase the intracellular Ca^{2+} concentration, which can enhance the forward-mode Na^{+}/Ca^{2+} exchanger (NCX) to promote inward current (I_{NCX}) in phase 2 of the action potential, resulting in the prolongation of J-T_{peak} and QT interval. RyR2: ryanodine receptor 2; and SR: sarcoplasmic reticulum.

Table 1. Drug-induced changes in the proarrhythmic surrogate markers along with their TdP risk categories

Drug	Dose	Proarrhythmic surrogate markers				References	TdP risk categories	
	(mg/kg, i.v.)	QTcV	J-T_{peak}c	T_{peak}-T_{end} (ms)	TRP (ms)		Chronic AV block dogs	CredibleMeds®
Antiarrhythmic agents								
E-4031	0.1	+94	+72	+38	+9	Izumi-Nakaseko et al., 2014*	High risk	N.A.
Vernakalant	3	+58	+26	+32	+9	Goto et al., 2023	N.A.	Possible Risk
Bepridil	3	+51	+31	+14	+4	Ishizaka et al., 2008*	Intermediate risk	Known Risk
Vanoxerine	0.3	+45	+36	+16	+13	Hagiwara-Nagasawa et al., 2021a	N.A.	N.A.
dl-Sotalol	3	+44	+35	+17	−1	Ishizaka et al., 2008*	High risk	Known Risk
Dronedarone	3	+41	+7	+28	+11	Motokawa et al., 2018	Low/No risk (tentative)	Known Risk
Ranolazine	3	+20	+11	+9	+11	Nunoi et al., 2021	N.A.	Conditional Risk
Amiodarone	3	+19	−10	+18	−11	Matsukura et al., 2017	Low/No risk	Known Risk
Tyrosine kinase inhibitors								
Imatinib	10	+29	+27	+3	+13	Chiba et al., 2022	N.A.	Possible Risk

Lapatinib	3	+18	+14	+1	+4	Ando et al., 2020*	Low/No risk (tentative)	Possible Risk
Sunitinib	0.1	+4	+12	−4	+6	Wada et al., 2018*	N.A.	Possible Risk
Dasatinib	0.3	+4	+1	−2	−2	Izumi-Nakaseko et al., 2020b	N.A.	Possible Risk
Antiviral drugs								
Amantadine	10	+42	+10	+33	+14	Cao et al., 2016	N.A.	Conditional Risk
Aciclovir	20	+35	−3	+30	+4	Kondo et al., 2020	N.A.	Not Classified
Peramivir	10	+20	+9	+13	+15	Kambayashi et al., 2024	N.A.	N.A.
Ivermectine	10	+20	+9	+12	+7	Suzuki et al., 2023	N.A.	Not Classified
Oseltamivir	30	+20	+4	+12	−4	Kitahara et al., 2013*	Low/No risk	Not Classified
Psychotropic drugs								
Paliperidone	3	+64	+11	+39	+12	Chiba et al., 2017	N.A.	Possible Risk
Donepezil	1	+42	+11	+31	−13	Hagiwara-Nagasawa et al., 2021b	Low/No risk	Known Risk
Perospirone	1	+28	−7	+32	+9	Kambayashi et al., 2020a	N.A.	N.A.
Lithium	10	+4	+3	0	+13	Goto et al., 2018b	N.A.	Possible Risk

Blonanserin	1	−4	+12	−11	−9	Kambayashi et al., 2020a	N.A.	N.A.
Memantine	1	−10	+7	−9	+4	Kambayashi et al., 2022a	N.A.	Not Classified

The values represent changes from each pre-drug basal control value after the drug/compound administration when the increment of QTcV was the greatest. TdP risk was referenced by the risk stratification based on our previous studies using the chronic atrioventricular (AV) block dogs (See Table 2 for more detail) or "QTDrugs List" of online resource CredibleMeds®. CredibleMeds TdP risk categories are as follows. Known risk: these drugs prolong QT interval, and are clearly associated with a known risk of TdP. Possible risk: these drugs can cause QT prolongation, but currently lack evidence for a risk of TdP. Conditional risk: these drugs are associated with TdP, but only under certain conditions of their use or by creating conditions that facilitate or induce TdP. Not classified: This drug has been reviewed by CredibleMeds, but the evidence available at this time did not result in a decision for it to be placed in any of the torsade risk categories. J-T_{peak}c: J-T_{peak} corrected with Johannesen's formula (Johannesen et al., 2014b); N.A.: not available; QTcV: QT interval corrected with Van de Water's formula (Van de Water et al., 1989); TdP: torsade de pointes; and TRP: terminal repolarization period. Asterisk (*) indicates that J-T_{peak}c and T_{peak}-T_{end} were re-calculated using original data.

Table 2. Risk stratification of drugs for the onset of TdP assessed by the conscious chronic atrioventricular block dogs

Risk for the onset of TdP	Drugs	≤3× of maximum clinical daily dose		>3× of maximum clinical daily dose		References
		Incidence of TdP	Drug doses	Incidence of TdP	Drug doses	
Cardiovascular agents						
High	Disopyramide	1/7	3 mg/kg/10 min, i.v.			Kambayashi et al., 2022b
	E-4031	0/4	0.03 mg/kg/10 min, i.v.			Goto et al., 2018a
		1/4	0.1 mg/kg/10 min, i.v.			
		4/4	0.3 mg/kg/10 min, i.v.			
	d-Sotalol	1/4	3 mg/kg, p.o.	4/4	30 mg/kg, p.o.	Goto et al., 2019a
	dl-Sotalol	3/4	3 mg/kg, p.o.			Goto et al., 2019a, 2019b
		3/4	10 mg/kg, p.o.			
Intermediate	Bepridil	0/4	3 mg/kg, p.o.	3/4	30 mg/kg, p.o.	Takahara et al., 2008
	Nifekalant	0/5	3 mg/kg, p.o.	5/5	30 mg/kg, p.o.	Satoh et al., 2004
	Sematilide	0/4	3 mg/kg, p.o.	3/4	30 mg/kg, p.o.	Yoshida et al., 2002

Low/No (tentative)	Amlodipine	0/8	2.5 mg/day for 28 days, p.o.			Takahara et al., 2009
	Aprindine	0/6	3 mg/kg/10 min, i.v.			Kambayashi et al., 2022b
	AVE0118	0/7	6 mg/kg/10 min, i.v.			Kambayashi et al., 2022b
	Candesaltan	0/7	12 mg/day for 28 days, p.o.			Takahara et al., 2009
	Cilnidipine	0/7	5 mg/day for 28 days, p.o			Takahara et al., 2009
	Cibenzoline	0/6	3 mg/kg/10 min, i.v.			Kambayashi et al., 2022b
	Dronedarone	0/4	3 mg/kg/30 s, i.v.			Karkhanis et al., 2022
	Pilsicainide	0/8	3 mg/kg/10 min, i.v.			Kambayashi et al., 2021a
	Poyendarone	0/4	3 mg/kg/30 s, i.v.			Karkhanis et al., 2022
Low/No	Amiodarone	0/4	3 mg/kg, p.o.	0/4	30 mg/kg, p.o.	Yoshida et al., 2002
		0/4	3 mg/kg/30 s, i.v.			Karkhanis et al., 2022
		0/4	200 mg/body for 7 days + 100 mg/body for following 21 days, p.o.			Takahara et al., 2008

Non-cardiovascular drugs

High	Cisapride	1/6	1 mg/kg, p.o.	6/6	10 mg/kg, p.o.	Sugiyama et al., 2002a
	Sulpiride	0/4	6 mg/kg, p.o.	2/4	120 mg/kg, p.o	Sugiyama et al., 2002c
		1/4	60 mg/kg, p.o.			
	Terfenadine	1/6	3 mg/kg, p.o.	5/6	30 mg/kg, p.o.	Takahara et al., 2006
Intermediate	Astemizole			0/4	3 mg/kg, p.o.	Izumi-Nakaseko et al., 2016
				1/4	30 mg/kg, p.o.	
	Gatifloxacin	0/4	10 mg/kg, p.o.	2/4	100 mg/kg, p.o.	Chiba et al., 2004
	Haloperidol			0/4	3 mg/kg, p.o.	Izumi-Nakaseko et al., 2017b
				4/4	30 mg/kg, p.o.	
	Moxifloxacin	0/4	10 mg/kg, p.o.	3/4	100 mg/kg, p.o.	Chiba et al., 2004
	Sparfloxacin	0/4	6 mg/kg, p.o.	4/4	60 mg/kg, p.o.	Chiba et al., 2000
Low/No (tentative)	Apomorphine	0/4	1 mg/kg/10 min, i.v.			Watanabe et al., 2015
	Azithromycin	0/4	30 mg/kg/10 min, i.v.			Ohara et al., 2015
	Kanzo	0/4	2 g/body for 3 days, p.o.			Izumi-Nakaseko et al., 2023a

		0/4	6 g/body for 3 days, p.o.			
	Lapatinib	0/4	3 mg/kg/10 min, i.v.			Ando et al., 2020
Low/No	Donepezil	0/4	0.1 mg/kg/10 min, i.v.	0/4	1 mg/kg/10 min, i.v.	Hagiwara-Nagasawa et al., 2021b
	Famotidine	0/4	1 mg/kg, p.o.	0/4	10 mg/kg, p.o.	Sugiyama et al., 2003
	Oseltamivir	0/4	3 mg/kg/10 min, i.v.	0/4	10 mg/kg/10 min, i.v.	Nakamura et al., 2016
	Levofloxacin	0/4	6 mg/kg, p.o.	0/4	60 mg/kg, p.o.	Chiba et al., 2000
	Risperidone			0/4	3 mg/kg/10 min, i.v.	Nunoi et al., 2020
	Sitafloxacin	0/4	10 mg/kg, p.o.	0/4	100 mg/kg, p.o.	Chiba et al., 2004

TdP: torsade de pointes

Table 3. Risk stratification of drugs for the onset of TdP assessed by the conscious chronic atrioventricular block monkeys

Risk for the onset of TdP	Drugs	≤3× of maximum clinical daily dose		>3× of maximum clinical daily dose		References
		Incidence of TdP	Drug doses	Incidence of TdP	Drug doses	
Antiarrhythmic agents						
High	*dl*-Sotalol	0/5	1 mg/kg, p.o.			Goto et al., 2021
		0/5	3 mg/kg, p.o.			
		5/5	10 mg/kg, p.o.			
Intermediate	Bepridil	0/4	10 mg/kg, p.o.	2/4	100 mg/kg	Goto et al., 2021
Low/No	Amiodarone			0/4	30 mg/kg, p.o.	Goto et al., 2022
	Verapamil	0/4	1.5 mg/kg, p.o.	0/4	15 mg/kg, p.o.	Goto et al., 2021
				0/4	75 mg/kg, p.o.	
Non-cardiovascular drugs						
Intermediate	Astemizole			0/6	1 mg/kg, p.o.	Goto et al., 2022
				3/6	5 mg/kg, p.o.	

				6/6	10 mg/kg, p.o.	
	Cisapride	0/6	1 mg/kg, p.o.	2/6	5 mg/kg, p.o.	Goto et al., 2021
	Haloperidol			0/5	1 mg/kg, p.o.	Goto et al., 2022
				1/5	10 mg/kg, p.o.	
				1/5	30 mg/kg, p.o.	
	Moxifloxacin	0/6	10 mg/kg, p.o.	0/6	30 mg/kg, p.o.	Goto et al., 2020b
				2/6	100 mg/kg, p.o.	
				1/6	60 mg/kg/2 h, i.v.	
				0/6	60 mg/kg/1 h, i.v.	
				3/6	120 mg/kg/2 h, i.v.	
Low/No	Famotidine			0/4	100 mg/kg, p.o.	Goto et al., 2022
	Levofloxacin			0/4	100 mg/kg, p.o.	Goto et al., 2022
	Terfenadine			0/4	30 mg/kg, p.o.	Goto et al., 2020a
	Tolterodine	0/4	0.2 mg/kg, p.o.	0/4	1 mg/kg, p.o.	Goto et al., 2022

		0/4	4 mg/kg, p.o.	
Drug interaction				
High (tentative)	Ketoconazole and terfenadine	4/4	100 mg/kg, p.o. ketoconazole followed by 30 mg/kg, p.o. terfenadine	Goto et al., 2020a

TdP: torsade de pointes

Table 4. A measurable incidence of cardiovascular drugs/compounds-induced TdP/risk by proarrhythmia models

			In silico, in vitro and ex vivo models				In vivo models			
Risk for the onset of TdP	Drugs	Human TdP risk categories	CiPA in silico model	iPS cell-derived cardiomyocyte sheet model	Langendorf-perfused isolated heart preparation	Arterially-perfused, ventricular wedge preparation	Conscious chronic AV block dogs	Anesthetized chronic AV block dogs	Acute AV block rabbits	Methoxamine-sensitized rabbits
High	Disopyramide	Known Risk	(H) Li et al., 2019	(+) Ando et al., 2017	(–) Lawrence et al., 2006	(H) Liu et al., 2021	(+) Kambayashi et al., 2022b			
	E-4031*			(+) Nakamura et al., 2014; (+) Ando et al., 2017; (+) Yamazaki et al., 2018	(+) Asano et al., 1997		(+) Goto et al., 2018a			(+) Buchanan et al., 1993

	d-Sotalol				(+) Sossalla et al., 2014; (–) Zabel et al., 1997	(+) Shimizu et al., 1999	(+) Goto et al., 2019a		(+) Thomsen et al., 2004		(+) Buchanan et al., 1993
	dl-Sotalol*	Known Risk	(H) Li et al., 2019	(+) Ando et al., 2017	(+) Guérard et al., 2008; (+) Lawrence et al., 2006	(+) Jia et al., 2011; (H) Liu et al., 2021	(+) Goto et al., 2019a; (+) Goto et al., 2019b	(+) Goto et al., 2021; (+) Izumi-Nakaseko et al., 2023b			
High (tentative)	Dofetilide	Known Risk	(H) Li et al., 2019	(+) Ando et al., 2017; (+) Yamazaki et al., 2018	(+) Steidl-Nichols et al., 2008; (+) Lawrence et al., 2006	(H) Liu et al., 2021			(+) Thomsen et al., 2006; (+) van Opstal et al., 2001a	(+) Hagiwara et al., 2017	(+) Lu et al., 2000; (+) Hagiwara et al., 2017

Intermediate	Bepridil*	Known Risk	(H) Li et al., 2019	(–) Ando et al., 2017; (–) Yamazaki et al., 2018	(+) Steidl-Nichols et al., 2008	(H) Liu et al., 2021	(+) Takahara et al., 2008	(+) Goto et al., 2021		
	Nifekalant	Known Risk					(+) Satoh et al., 2004		(+) Kawakami et al., 2022; (+) Kawakami et al., 2023	(+) Inaba et al., 2008
	Sematilide			(–) Ando et al., 2017			(+) Yoshida et al., 2002			(+) Carlsson et al., 1990
Low/No (tentative)	Amlodipine	Not Classified			(–) Lawrence et al., 2006		(–) Takahara et al., 2009			
	Aprindine						(–) Kambayashi			

				et al., 2022b	
AVE0118				(–) Kambayashi	(–) Kambayashi
				et al., 2022b	et al., 2020b; (–)
					Oros et al., 2006
Candesaltan				(–) Takahara et	
				al., 2009	
Cilnidipine				(–) Takahara et	
				al., 2009	
Cibenzoline			(+) Lawrence et	(–) Kambayashi	
			al., 2006	et al., 2022b	
Dronedarone*	Known	(–) Ando et al., 2017		(–) Karkhanis et	(+) van Opstal et
	Risk			al., 2022	al., 2001b; (–)
					Kambayashi et
					al.,2021b

	Pilsicainide	Possible Risk				(–) Kambayashi et al., 2021a		(–) Iwasaki et al., 2009		
	Poyendarone					(–) Karkhanis et al., 2022		(–) Kambayashi et al., 2021b		
Low/No	Amiodarone*	Known Risk		(–) Ando et al., 2017; (–) Yamazaki et al., 2018	(–) Zabel et al., 1997; (–) Hondeghem and Hoffmann, 2003	(–) Sicouri et al., 1997	(–) Yoshida et al., 2002; (–) Karkhanis et al., 2022; (–) Takahara et al., 2008	(–) Goto et al., 2022	(–) van Opstal et al., 2001b	(–) Hagiwara et al., 2017
	Verapamil	Not Classified	(L) Li et al., 2019	(–) Ando et al., 2017	(–) Tabo et al., 2010; (–) Hondeghem and Hoffmann, 2003;	(L) Liu et al., 2021		(–) Goto et al., 2021	(–) Bourgonje et al., 2013; (–) Oros et al., 2010	

(–) Steidl-Nichols

et al., 2008

“Risk for the onset of TdP" is based on the results of conscious chronic AV block dogs and monkeys (Tables 2 and 3). Asterisk (*) indicates that information of the proarrhythmic surrogate markers is provided in Table 1. As for “Human TdP risk categories”, see Table 1 legend for more information, which are based on CredibleMeds® TdP risk categories. If the model detects drug-induced TdP, it is marked (+); if not, it is marked (–). In CiPA in silico model (Li et al., 2019) and arterially-perfused, ventricular wedge preparation (Lu et al., 2007; Liu et al., 2021), TdP risk of a drug is classified into low (L), intermediate (I) and high (H) according to torsade metric score and TdP risk score, respectively. In iPS cell-derived cardiomyocyte sheet model, when early afterdepolarization is induced, it is marked (+); if not, it is marked (–). While no cardiovascular drug-induced TdP has been reported for chronic AV block rabbit model, sematilide induced TdP in blood-perfused, ventricular muscle preparation (Sugiyama and Hashimoto, 2002) and dofetilide did it in genetically engineered rabbit LQT5 model (Major et al., 2016), which are not indicated in Table 4. AV: atrioventricular; CiPA: comprehensive in vitro proarrhythmia assay; iPS: induced pluripotent stem; and TdP: torsade de pointes.

Table 5. A measurable incidence of non-cardiovascular drugs-induced TdP/risk by proarrhythmia models

			In silico, in vitro and ex vivo models				In vivo models				
Risk for the onset of TdP	Drugs	Human TdP risk categories	CiPA in silico model	iPS cell-derived cardiomyocyte sheet model	Langendorf-perfused isolated heart preparation	Arterially-perfused, ventricular wedge preparation	Conscious chronic AV block dogs	Conscious chronic AV block monkeys	Anesthetized chronic AV block dogs	Acute AV block rabbits	Methoxamine-sensitized rabbits
High	Cisapride	Known Risk	(I) Li et al., 2019	(+) Ando et al., 2017; (+) Yamazaki et al., 2018	(+) Steidl-Nichols et al., 2008	(+) Di Diego et al., 2003; (I) Liu et al., 2021	(+) Sugiyama et al., 2002a	(+) Goto et al., 2021	(+) Vos 2008		(+) Carlsson et al., 1997
	Sulpiride	Known Risk					(+) Sugiyama et al., 2002c				
	Terfenadine	Known Risk	(I) Li et al., 2019	(–) Ando et al., 2017	(+) Hondeghem and Hoffmann, 2003; (–	(I) Liu et al., 2021	(+) Takahara et al., 2006	(+) with ketoconazole; (–) Goto et al.,			(–) Lu et al., 2000: (–) Batey and Coker,

					Steidl-Nichols et al., 2008			2020a			2002
Intermediate	Astemizole	Known Risk	(I) Li et al., 2019	(+) Ando et al., 2017; (+) Yamazaki et al., 2018	(+) Steidl-Nichols et al., 2008	(I) Liu et al., 2021	(+) Izumi-Nakasek o et al., 2016	(+) Goto et al., 2022			
	Gatifloxacin	Known Risk		(+) Ando et al., 2017			(+) Chiba et al., 2004				(+) Chiba et al., 2004; (+) Akita et al., 2004
	Haloperidol	Known Risk		(+) Ando et al., 2017	(+) Hondeghem & Hoffmann, 2003; (+) Steidl-Nichols et al., 2008		(+) Izumi-Nakasek o et al., 2017b	(+) Goto et al., 2022		(+) Hagiwara et al., 2017	
	Moxifloxacin	Known Risk		(–) Ando et al., 2017; (–) Yamazaki	(–) Tabo et al., 2010; (+)	(–) Chen et al., 2005;	(+) Chiba et al., 2004	(+) Goto et al., 2020b	(–) Thomsen et al., 2006	(–) Hagiwara et	(–) Anderson et al., 2001; (–)

			et al., 2018	Steidl-Nichols et al., 2008; (+) Lu et al., 2007	(H) Lu et al., 2007			al., 2017	Chiba et al., 2004
	Sparfloxacin	Known Risk	(+) Ando et al., 2017	(–) Lu et al., 2007	(H) Lu et al., 2007	(+) Chiba et al., 2000		(+) Hagiwara et al., 2017	(+) Anderson et al., 2001; (+) Akita et al., 2004
Low/No (tentative)	Apomorphine	Possible Risk				(–) Watanabe et al., 2015			
	Azithromycin	Known Risk	(–) Delaunois et al., 2021	(–) Milberg et al., 2002; (+) Lawrence et al., 2006		(–) Ohara et al., 2015	(–) Thomsen et al., 2006		
	Kanzo		(–) Izumi-Nakaseko			(–)			

			et al., 2023a		Izumi-Nakaseko et al., 2023a	
	Lapatinib*	Possible Risk			(–) Ando et al., 2020	
Low/No	Donepezil*	Known Risk		(+) Ellermann et al., 2020	(–) Hagiwara-Nagasawa et al., 2021b	
	Famotidine	Condition al Risk	(–) Ando et al., 2017		(–) Sugiyama et al., 2003	(–) Goto et al., 2022
	Oseltamivir*	Not Classified			(–) Nakamura et al., 2016; (–) Kambayashi et al., 2021a	(–) Kambayashi et al., 2022c

Levofloxacin	Known Risk			(+) Milberg et al., 2007		(–) Chiba et al., 2000	(–) Goto et al., 2022		(–) Akita et al., 2004
Risperidone	Condition al Risk	(I) Li et al., 2019	(+) Ando et al., 2017; (–) Yamazaki et al., 2018	(+) Steidl-Nichols et al., 2008	(I) Liu et al., 2021	(–) Nunoi et al., 2020		(+) Hagiwara et al., 2016	
Sitafloxacin	Not Classified					(–) Chiba et al., 2004			(–) Chiba et al., 2004
Tolterodine	Possible Risk		(+) Ando et al., 2017				(–) Goto et al., 2022		

"Risk for the onset of TdP" is based on the results of conscious chronic AV block dogs and monkeys (Tables 2 and 3). Asterisk (*) indicates that information of the proarrhythmic surrogate markers is provided in Table 1. As for "Human TdP risk categories", see Table 1 legend for more information, which are based on CredibleMeds® TdP risk categories. If the model detects drug-induced TdP, it is marked (+); if not, it is marked (–). In CiPA in silico model (Li et al., 2019) and arterially-perfused, ventricular wedge preparation (Lu et al., 2007; Liu et al., 2021), TdP risk of a drug is classified into low (L), intermediate (I) and high (H) according to torsade metric score and TdP risk score, respectively. In iPS cell-derived cardiomyocyte sheet model, when early afterdepolarization is induced, it is marked (+); if not, it is marked (–). Non-cardiovascular drugs-induced TdP has not been reported for blood-perfused, ventricular muscle

preparation, chronic AV block rabbit model or genetically engineered rabbit models, which are not indicated in Table 5. AV: atrioventricular; CiPA: comprehensive in vitro proarrhythmia assay; iPS: induced pluripotent stem; and TdP: torsade de pointes.

Fig. 1

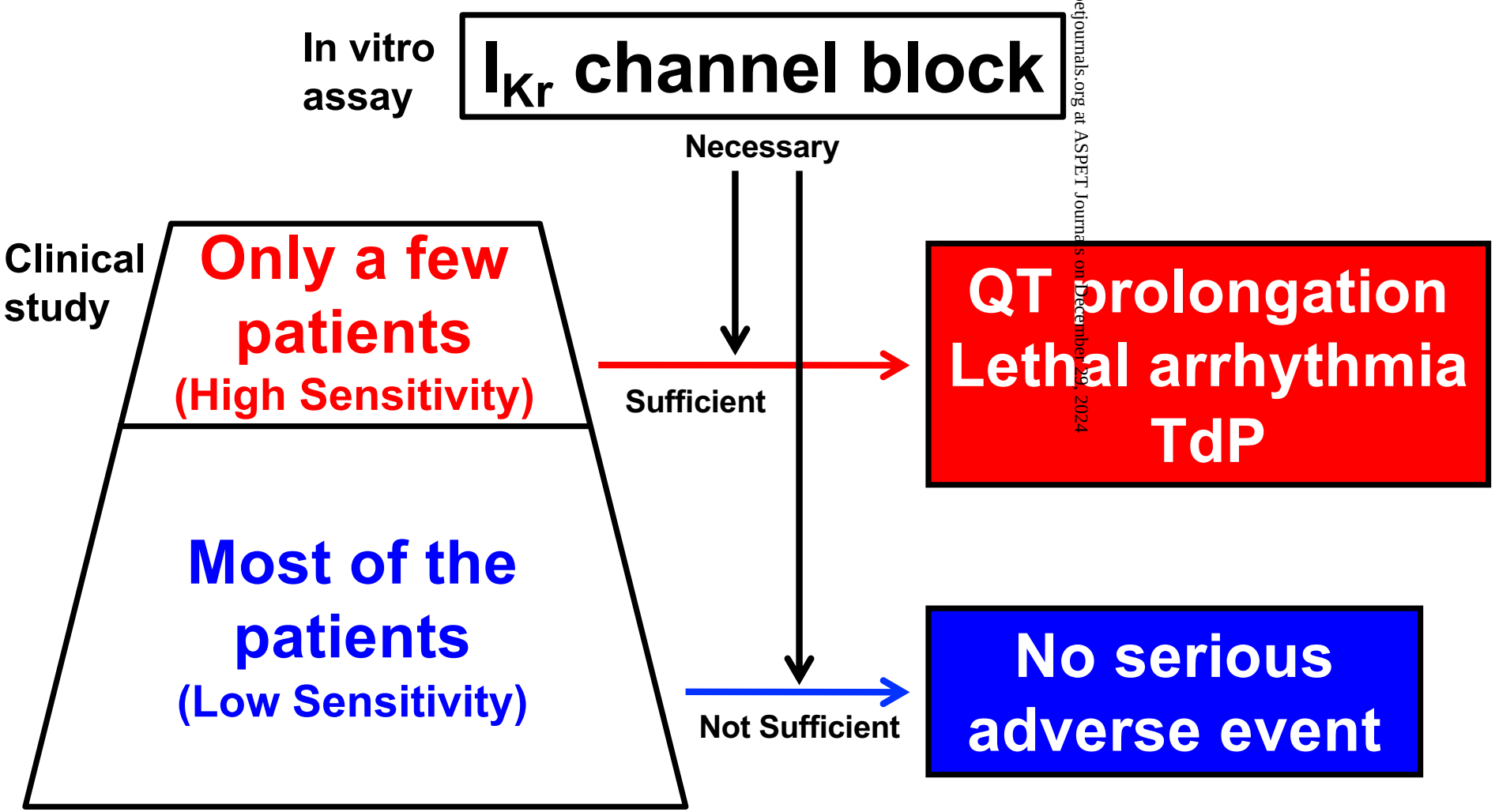

Fig. 2

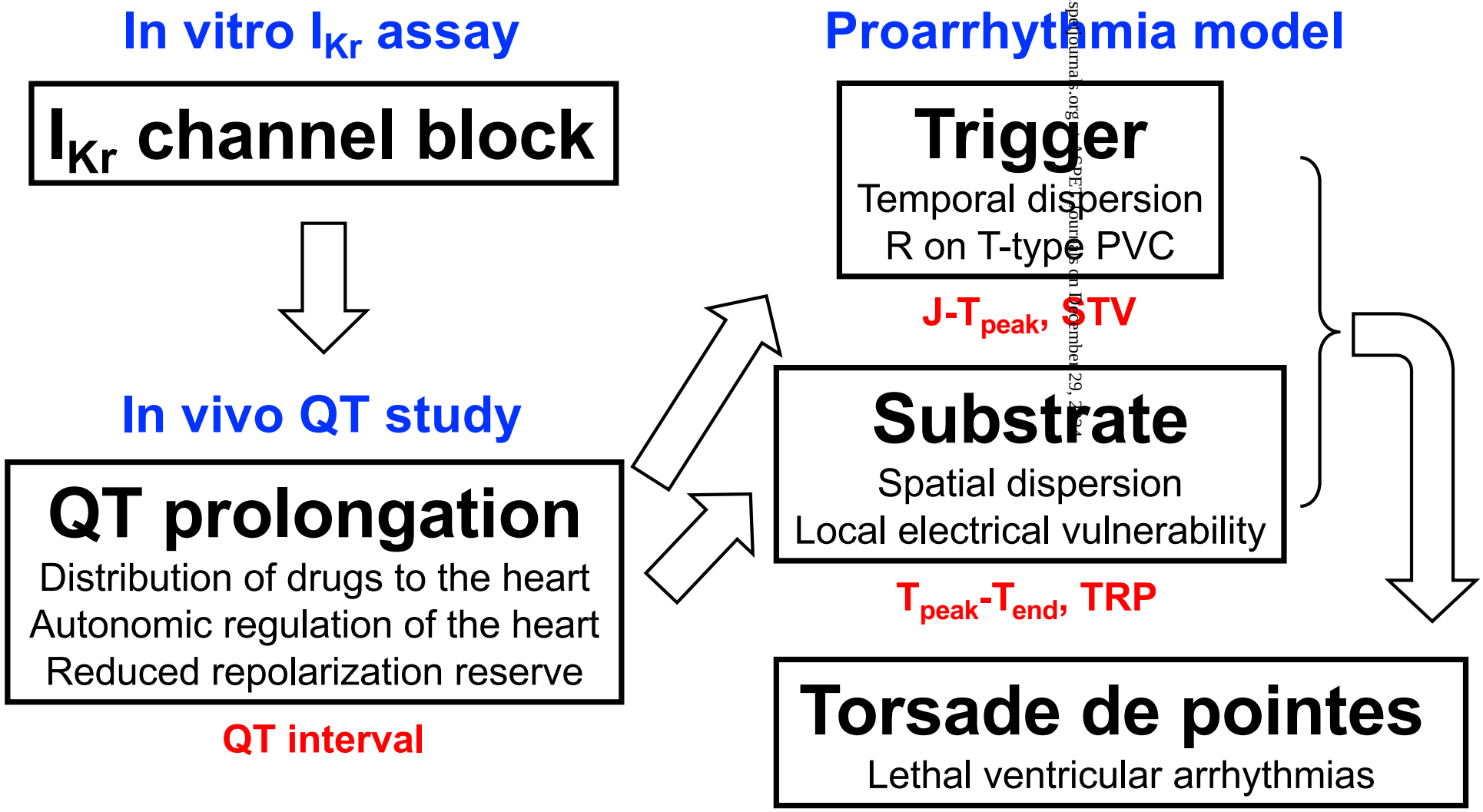

Fig. 3

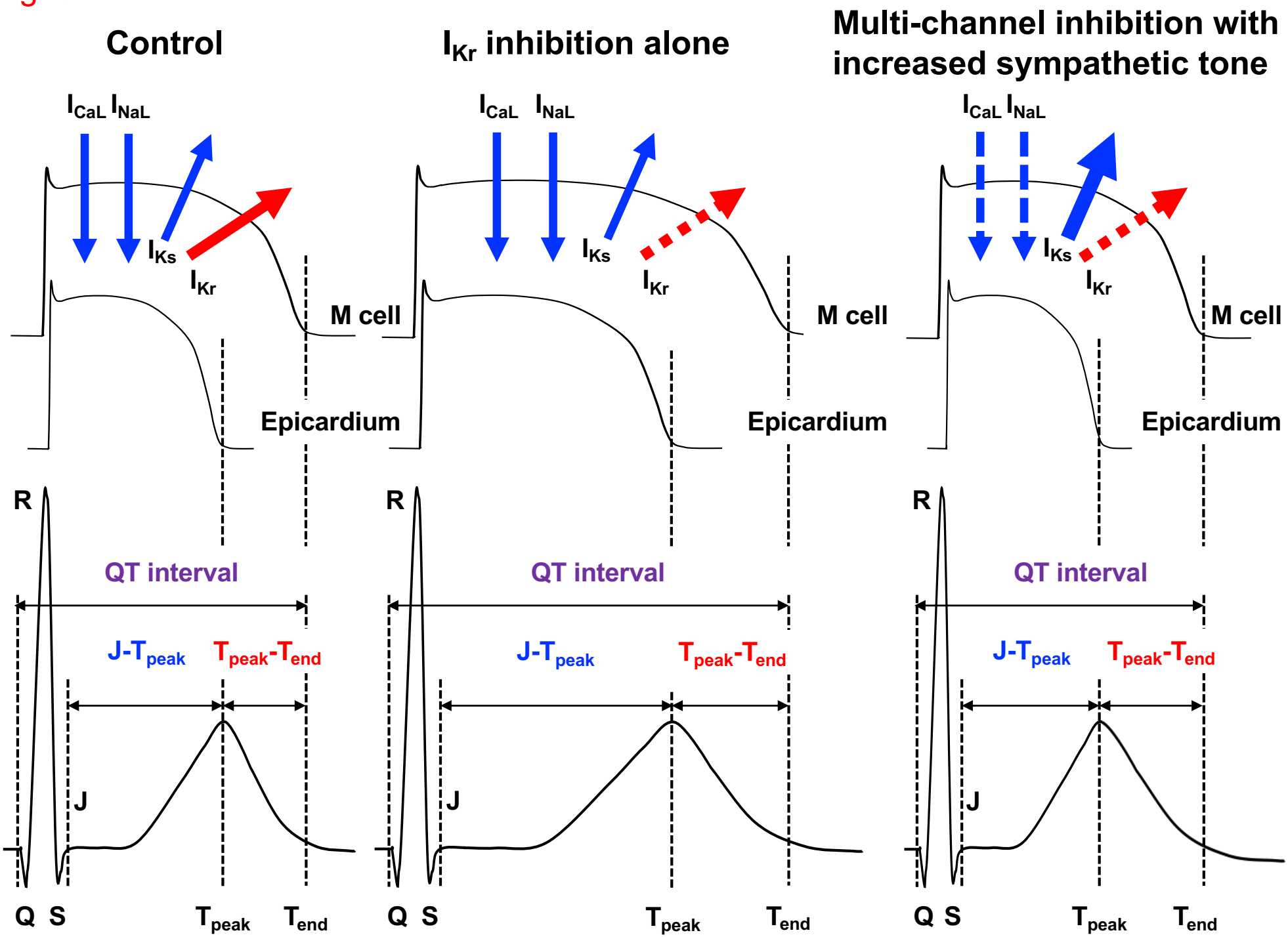
Control
I_{Kr} inhibition alone
Multi-channel inhibition with increased sympathetic tone
I_{CaL} I_{NaL}
I_{Ks}
I_{Kr}
M cell
Epicardium
R
QT interval
$J\text{-}T_{peak}$
$T_{peak}\text{-}T_{end}$
J
Q S
T_{peak}
T_{end}

Fig. 4

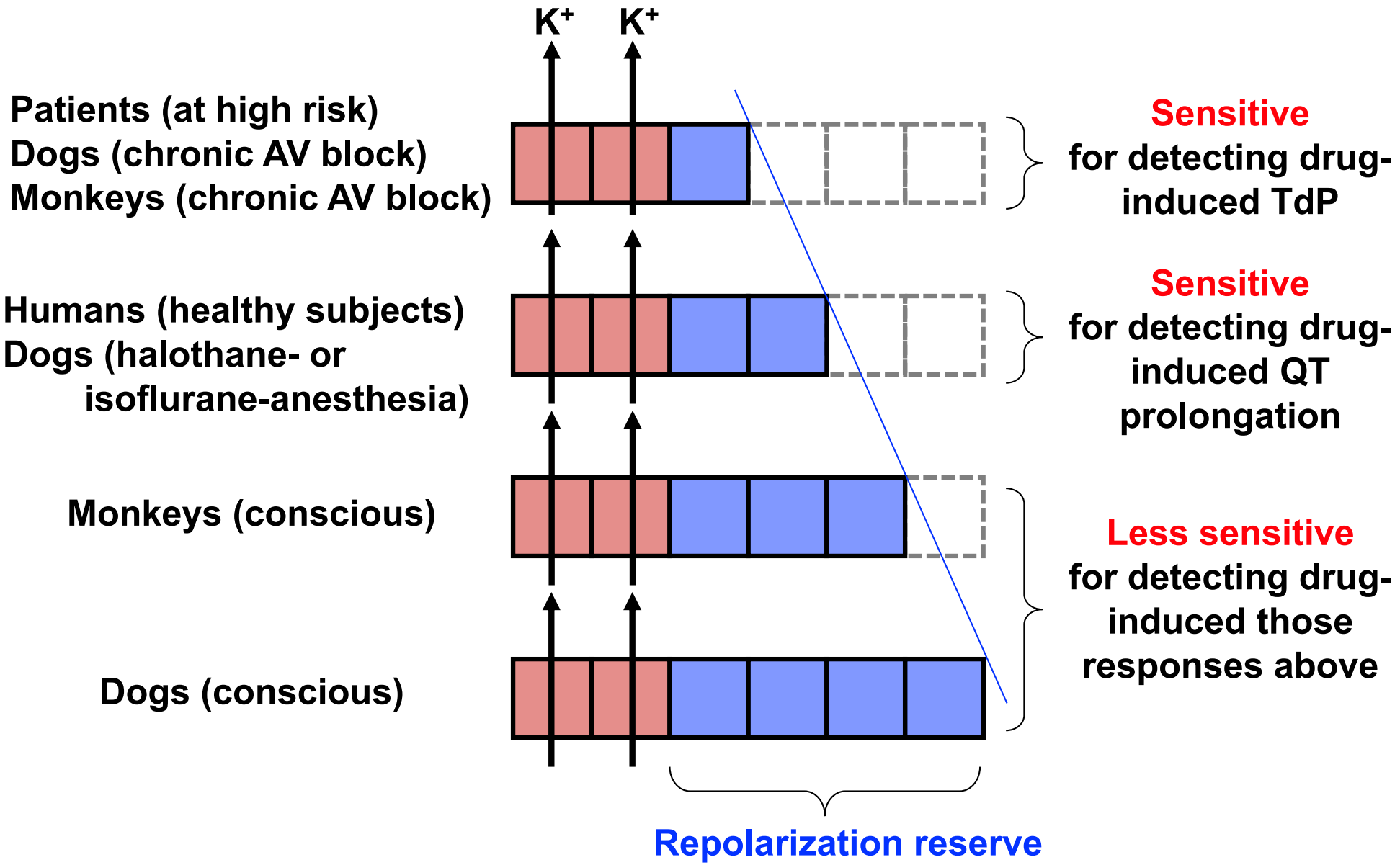
K+
K+
Patients (at high risk)
Dogs (chronic AV block)
Monkeys (chronic AV block)
Sensitive
for detecting drug-induced TdP
Humans (healthy subjects)
Dogs (halothane- or isoflurane-anesthesia)
Sensitive
for detecting drug-induced QT prolongation
Monkeys (conscious)
Dogs (conscious)
Less sensitive
for detecting drug-induced those responses above
Repolarization reserve

Fig. 5

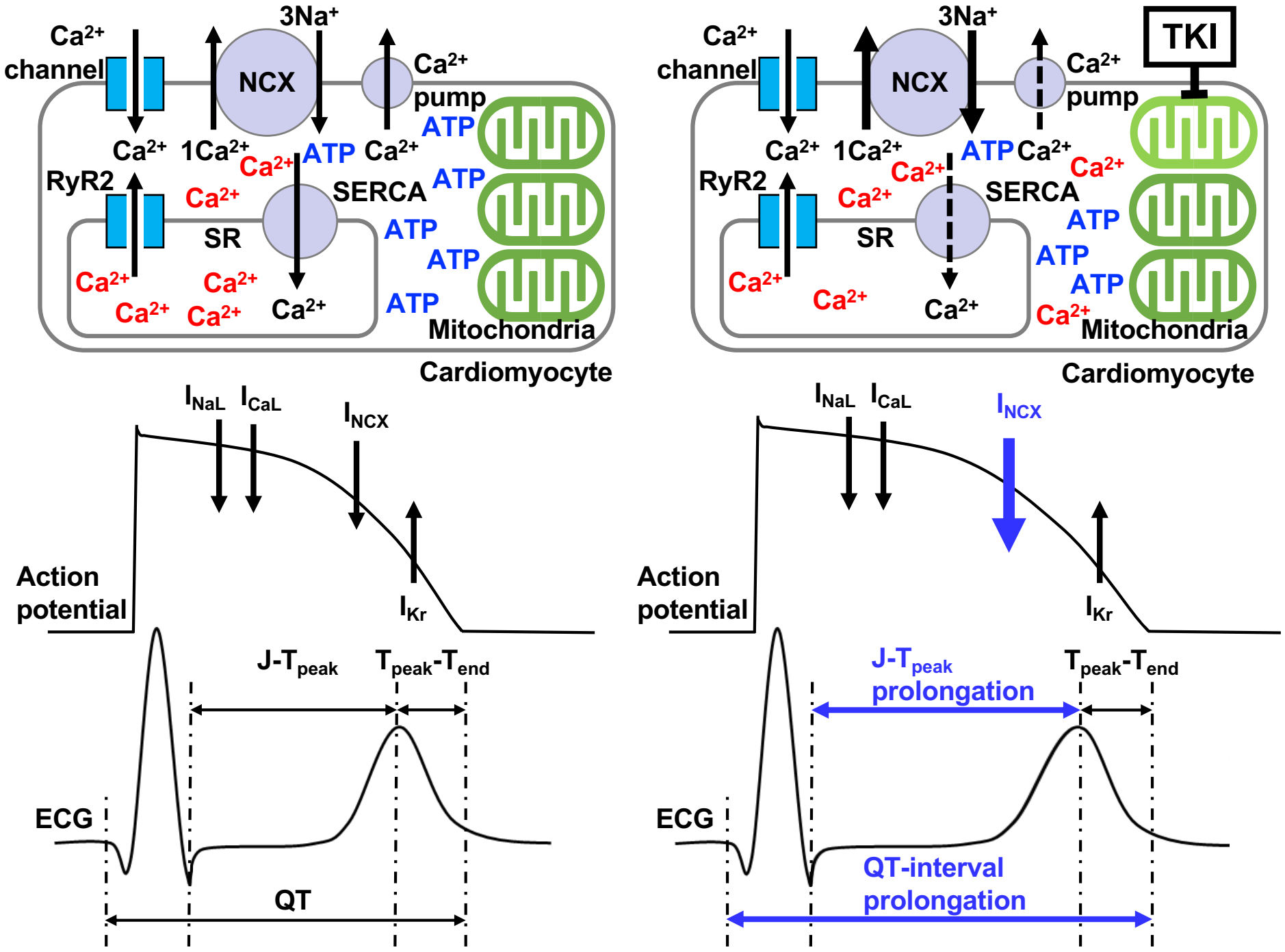
Ca2+ channel
3Na+
NCX
Ca2+ pump
Ca2+
1Ca2+
ATP
Ca2+
RyR2
Ca2+
SERCA
SR
ATP
ATP
ATP
Ca2+
Ca2+
Ca2+
Ca2+
Ca2+
Mitochondria
Cardiomyocyte
TKI
INaL
ICaL
INCX
IKr
Action potential
J-Tpeak
Tpeak-Tend
ECG
QT
J-Tpeak prolongation
QT-interval prolongation